NOVA SCHOOL OF SCIENCE & TECHNOLOGY

DEPARTAMENT OF
Physics

# Comparison of Therapeutic Delivery Efficacy of Different EV Subpopulations

Raul Alexandre Mota Leandro
BSc in Biochemistry

MASTER IN Biomaterials and Nanomedicine
NOVA University Lisbon
September, 2023

NOVA SCHOOL OF SCIENCE & TECHNOLOGY

DEPARTAMENT OF
Physics

# Comparison of Therapeutic Delivery Efficacy of Different EV Subpopulations

**Raul Alexandre Mota Leandro**

Master in Biomaterials and Nanomedicine

**Adviser:** Pedro Baptista
*Full Professor, NOVA University Lisbon*

**Co-advisers:** Sander Kooijmans
Post-Doc, UMC Utrecht

**Examination Committee:**

**Chair:** Name of the committee chairperson,
Full Professor, FCT-NOVA

**Rapporteurs:** Name of a rapporteur,
Associate Professor, Another University
Name of another rapporteur,
Assistant Professor, Another University

**Adviser:** Name of the adviser present in defense,
Associate Professor, University

**Members:** Yet another member of the committee,
Full Professor, Another University
Yet another member of the committee,
Assistant Professor, Another University

MASTER IN Biomaterials and Nanomedicine

NOVA University Lisbon
September, 2023

**Comparison of Therapeutic Delivery Efficacy of Different EV Subpopulations**

To my family and friends.

# ACKNOWLEDGMENTS

I would like to start by thanking Professor Pedro Baptista (Universidade Nova de Lisboa) for accepting to be my coordinator and helping with the bureaucracy for the Erasmus.
I would also like to thank Dr. Raymond Schiffelers and Dr. Pieter Vader for accepting me in their laboratory with great hospitality. I also want to express my gratitude for Dr. Sander Kooijmans for being my supervisor through all my work and helping me develop my skills in the laboratory.
I would like to thank other students of the CDL such as, Mafalda Cabana, Tanya Karakyriakou, Zoë Eeckhout, Maryse Boess, for always keeping me company and making me laugh.
Thank you Naomie Zhou, Mariu Laura Tognoli and Jerney François for guiding me through some experiences and always answering my questions.
A big thank you to all the CDL (UMC Utrecht) for providing such a nice environment to work and learn.
A big thank you to my girlfriend Jonie Verdonck, who i met during my Erasmus thesis, for all the emotional support, help in improving my English writing skills and always making my day better.
Thank you people living in the biltstraat residency for the 9 months who made my days fun and bright and which I will cherish for all my life.
Lastly, I want to thank my family, for the emotional, financial support and always believing in me.

"What is not started will never get finished." (Johann Wolfgang Goethe).

# ABSTRACT

In the last decades, RNA therapeutics have been brought to light by the ability to silence or activate gene expression. However, RNA is degraded in bodily fluids and does not permeate the hydrophobic cell membranes, being necessary to use RNA carriers that can safely deliver it to the cells while maintaining its function.

Extracellular vesicles (EVs) are secreted by the cells and recognized as natural information carriers within the body. They facilitate the RNA delivery between cells and hold the potential for utilization as therapeutic delivery systems. EVs are highly heterogeneous, featuring various subpopulations formed in different biogenesis pathways. This heterogeneity of EVs results in different functions driven by the proteins present on their surface, enabling them to target different cell types and evoke different cellular responses. As such, it would be important to compare the EV-mediated RNA delivery of the different subpopulations. However, the study of the different subpopulations is challenging, due to the lack of isolations methods for EV subpopulations based on their surface molecules.

The aim of this work was to compare the efficiency of the EV-mediated RNA delivery of different EV subpopulations. HEK293T cells were engineered to express a recombinant protein for loading of a sgRNA and Cas9 in the EVs for activation of the reporter system. The EV subpopulations were isolated in an immunoprecipitation with magnetic beads and added to reporter cells of the reporter system. This system allowed the analysis of the EV-mediated RNA delivery by the expression of eGFP when the cells received the sgRNA and Cas9 loaded to the EVs. In all assays done CD9+ and CD81+ subpopulations were the most potent at delivering the cargo. Consequently, investigation of the subpopulations holds significant importance in advancing the development of therapeutic delivery systems.

**Keywords**: Extracellular vesicles, Extracellular vesicles subpopulations, RNA, CROSS-FIRE system.

# RESUMO

Nas últimas décadas, têm vindo a ser desenvolvidas terapias de RNA devido à sua capacidade de ativar, silenciar ou editar genes. No entanto, o RNA é degradado nos fluidos corporais e não permeia as membranas celulares hidrofóbicas, sendo necessário utilizar transportadores que possam entregar o RNA às células, mantendo a sua função.

As vesículas extracelulares (EVs) são segregadas pelas células e reconhecidas como transportadores naturais de informação dentro do organismo, facilitando a entrega de RNA entre as células e com potencial para serem utilizadas como sistemas de vectroização terapêutica. As EVs são altamente heterogéneas, apresentando várias subpopulações formadas em diferentes vias de biogénese. Esta diversidade de EVs resulta em diferentes funções determinadas pelas proteínas presentes na sua superfície, permitindo-lhes visar diferentes tipos de células e evocar distintas respostas celulares. Como tal, é importante comparar a entrega de RNA mediada por EVs das diferentes subpopulações. No entanto, o estudo das diferentes subpopulações é difícil, uma vez que não existem métodos de isolamento das subpopulações de EV com base nas suas moléculas de superfície.

O objetivo deste trabalho foi comparar a eficiência da entrega de RNA mediada por EVs de diferentes subpopulações. As células HEK293T foram concebidas para expressar uma proteína recombinante para carregar um sgRNA e Cas9 nos EVs para ativação do sistema repórter. As subpopulações de EVs foram isoladas numa imunoprecipitação com esferas magnéticas e adicionadas às células repórteres do sistema. Este sistema permitiu a análise da entrega de RNA mediada por EV através da expressão de eGFP quando as células receberam o sgRNA e Cas9 carregados nos EVs. Em todos os ensaios efetuados, as subpopulações CD9+ e CD81+ foram as mais eficientes na entrega da carga. A continuada investigação das subpopulações tem uma importância significativa no avanço do desenvolvimento de sistemas de entrega terapêutica.

**Palavras-chave:** Vesículas extracelulares, Subpopulações de vesículas extracelulares, RNA, sistema CROSS-FIRE.

# CONTENTS

# LIST OF FIGURES

# LIST OF TABLES

# ACRONYMS

| | |
|---|---|
| **Alix** | Programmed cell death 6-interacting protein |
| **CPC** | Cardiac progenitor cell |
| **CRISPR** | clustered regularly interspaced short palindromic repeats |
| **CROSS-FIRE** | CRISPR Operated Stoplight System for Functional Intercellular RNA Exchange |
| **crRNA** | CRISPR RNA |
| **DNA** | Deoxyribonucleic acid |
| **DTT** | Dithiothreitol |
| **EV** | Extracellular Vesicle |
| **FCS** | Fetal Calf Serum |
| **GFP** | Green Fluorescence Protein |
| **HA** | Human influenza hemagglutinin |
| **hEGF** | Human Epidermal growth factor |
| **HEK** | Human Embryonic Kidney |
| **HMEC** | Human Mammarian Epithelial cell |
| **HSC70** | heat shock cognate 70 |
| **HSP70** | Heat shock protein 70 |
| **MVE** | Multivesicular endosomes |
| **NTA** | Nanoparticle Tracking analysis |
| **PBS** | Phosphate buffered saline |

| | |
|---|---|
| **PBSA** | PBS with 1% Bovise Serum Albumin |
| **PBS-T** | PBS 0.001% v/v Tween20 |
| **PD** | Pulldown |
| **PEI** | Polyethylenimine |
| **PS** | phosphatidylserine |
| **PVDF** | Polyvinylidene Fluoride |
| **P/S** | Penicilin and Streptomycin |
| **RFP** | Red Fluorescence Protein |
| **RNA** | Ribonucleic Acid |
| **RT** | Room Temperature |
| **sEV** | Small extracellular vesicles |
| **sgRNA** | Single-Guide Ribonluciec acid |
| **SHOBS** | Sodium Hydrogen Orthophosphate Buffered Saline buffer |
| **SP** | Supernatant |
| **TBS** | Tris Buffered Saline |
| **TE** | Tripsin/EDTA |
| **tracrRNA** | Trans-activating CRISPR RNA |
| **TSG101** | Tumor susceptibility gene protein 101 |
| **UV** | Ultraviolet |
| **VSV-G** | Vesicular stomatitis virus glycoprotein |

# 1

# INTRODUCTION

Intercellular communication has an important role in the maintenance of homeostasis and in providing efficient response to threats of the surrounding environment[1]. Intercellular communication can occur in diverse ways by the delivery of nucleic acids, proteins and lipids between cells. The body has evolved to optimize the communication between cells, enabling efficient signaling, optimal for the response needed. The understanding of these complex types of signaling would help to understand how some diseases can affect the human body, and improve their treatment. An example is how cancer cells dispose of chemotherapeutic agents and other toxic molecules by encapsulating them in extracellular vesicles[1,2]. These pathways and signaling would also allow the development of new therapeutic agents or delivery agents, which could improve the treatment of different pathologies[3]. The use of ribonucleic acids (RNA) therapeutics is a flourishing area in the past decades, because of the possibility of targeting genes, RNAs and protein expression to treat different diseases or reduce the expression of symptoms[1,4–8]. These therapeutics present big versatility as they allow different pathways and molecules to be targeted comparing to the small molecule drugs that overrun the market[3]. One of the most observed ways for the delivery of active content in the body is by extracellular vesicles (EVs). They were first described as a part of a system for removal of toxic components of cells, but in recent years, they have been gaining the interest of the science community for their possible use as drug delivery systems[9,10]. EVs are natural cargo carriers, delivering RNA, proteins and nucleic acids to other cells. Their use could be a great improvement to the current drug delivery systems, which are based on synthetic lipid carriers[5–7,11,12].

## 1.1 RNA Therapeutics

When it was first discovered, RNA was believed to be only a mean to carry information from DNA to protein, however in the last decade, the possibilities of RNA have been further researched[8]. RNA therapeutics consist of broad variety of polymers such as antisense oligonucleotides, aptamers, small interference RNA and single guide RNA[13]. Different RNA therapeutics have already been developed and are present in the market, such as the RNA COVID-19 vaccine, the CRISPR/Cas9 gene editing technique that has already been used to treat life-threatening diseases and modify embryo cells[8,14,15]. In the last decades, RNA therapeutics have been gaining a great interest by the science community as substitute for small molecule drugs which govern the current market, as the typical drugs present a small-term effect and mostly inhibits proteins[8]. Nucleic acids present the ability for gene editing, inhibition and expression of ribonucleic acids or deoxyribonucleic acids (DNA) as therapeutic effect. These therapeutics present advantages compared to small molecule drugs. While small molecules can inhibit multiple molecules at once, nucleic acids allow for a targeted treatment for genetic diseases by the inhibition of gene expression or the upregulation of the gene. This research brought the use of RNA for treatment of diseases to light[4,8,13,16].

### 1.1.1 CRISPR/Cas9

The clustered, regularly interspaced, short palindromic repeats (CRISPR) and the associated protein Cas, provides defense to viruses and plasmids to prokaryotes. This allows for a great immunity response by being able to identify external DNA that is inserted[17]. If the prokaryotes were previously infected with the same DNA, it will recognize the sequence, by the association of a CRISPR RNA (crRNA) produced in a previous invasion of the host. The association with another trans-activating CRISPR RNA (tracrRNA) forms a guide RNA that will specifically cleave foreign DNA sequences and protect the host[16,17]. The use of the programmable nuclease Cas9 allows for the use of any desired single guide RNA (Association of both CRISPR RNA) for efficient genome editing. In the last decade, this system has been getting recognition for the potential for gene editing, since by manipulation of the sgRNA the specificity of the targeting can be altered[15–17]. By synthetic creation of the sgRNA by transcription of the desired targeted DNA we are able to specifically target the sequence, causing a frameshift which can alter the readout of the DNA[17].

### 1.1.2 RNA Delivery

As previously stated in 1.1, nucleic acid therapeutics presents great advantages compared to the products considered the standard in the market. Nonetheless, the use of nucleic acid for

therapeutics presents issues that are necessary to overcome. RNases are present in all body fluids not allowing the use of free nucleic acids therapeutics in the body, apart from the poor permeability for hydrophobic membranes[5,7]. An efficient delivery of the therapeutic nucleic acid is necessary for functionality. Lipid nanoparticles emerged as promising nucleic acid carriers as they presented high versatility in their functionality, and even extended to other fields such as medical imaging, cosmetic and others[14]. For nucleic acid delivery, different lipids uses are already on the market such as the current COVID-19 mRNA vaccines that, with the use of lipids to increase the lifetime in circulation promoted an efficient and intact delivery of the RNA[14]. Liposomes were the early version of lipid nanoparticles and still the most commonly used as they are versatile carriers, easily manipulated to the desired properties and present the ability carry both hydrophobic and hydrophilic drugs or small molecules such as proteins and nucleic acids[14,18]. Liposomes were also able to respond to the necessities that were lacking for nucleic acid therapies, protecting the active content enzymes, improving the pharmacokinetic profile, improve drug targeting while reducing the possibility of side effects [14,18]. However, lipid nanoparticles are synthetic carriers in which is necessary to add targeting molecules while they may still lack specific biodistribution in the body and may cause an immune response[14,18,19].

In recent years the study of intercellular communication brought to light the applicability of EVs, natural carriers of cargo such as proteins and nucleic acids in the body[20]. EVs are produced by all cells in the body, and used as a natural carrier of active content for intercellular communication[13]. Vesicles also may present some benefits as an alternative carrier for drug delivery systems compared to the preferred lipid nanoparticles in the market, as it has natural innate targeting specificity, comparing to the synthetic targeting of lipid nanoparticles, and lack toxicity and immunogenicity[13,21]. Apart from that, EVs associated proteins may also present intrinsic advantages as they can promote angiogenesis, cell proliferation and cell migration[22,23].

The study of RNA delivery systems, presents a major drawback which is the inability of phenotypically distinguish if the activation of the system is done by the RNA delivered or the delivery of the translated protein[24]. To overcome this issue different methods have been designed to study the functional delivery of the RNA independent of the protein translated. A technique suitable for such analysis is the CRISPR/Cas9 system since it could be used to change the phenotype of the cell which is directly dependent of the delivery of the Cas9/sgRNA complex to the nucleus, hence it would be a great technique to overcome the major drawbacks of RNA delivery studies[25].

## 1.2 Extracellular Vesicles

EVs are the natural messengers in the body for intercellular communication with a varying size between 50-1000nm of diameter. Extracellular vesicles is a broad generic name for all vesicles secreted by cells that are highly heterogeneous as EVS can present two different patways of biogenesis. When they are formed by the maturation of multivesicular endosomes (MVEs) and no fusion with the lysosomes occurs, the vesicles will fuse with the plasma membrane and be released to the extracellular space. This vesicles are called exossomes (30-100nm) [7,9,11,12]. When they are formed by the budding of the plasma membrane, which can occur via ESCRT dependent and independent pathways and named microvesicles (50-1000nm) [7,9,11,12,24].. Apoptotic bodies are the largest vesicles with a size over 500nm and are formed when programmed cell death occurs[7,9,11,12,24].

EVs were initially considered to be the garbage bins of the cells, used to dispose of organelles and molecules toxic for the cells, which has been shown to occur in different cells and dependent on the situation[10]. In the last decade, they have been further recognized and investigated by the community by their multiple functionalities, however, most of their functions remain undiscovered. EVs were brought to light by their potential as natural drug carriers, as in the body, cells secrete thousands of vesicles and use them for intercellular communication by endocrine, paracrine pathways[26,27]. The great interest was mostly by the first discovers on how EVs could functionally transfer different types of RNA such as mRNA, miRNA and more with possible important role for different pathologies[19,28,29]. This knowledge opened the possibility to use engineered EVs for delivery of engineered RNAs for treatment of different diseases. EVs are able to reach distant cells from the donor and deliver intact active content to the receptor cells, where they attach either by recognition of ligand/receptor in the EV and cell surface respectively, or EV fusion directly with the membrane[30]. Uptake of EVs usually occurs by endocytosis, has shown in the literature by the reduction of EV uptake when molecules related to endocytosis pathway are silenced[31].

Despite the blooming of the EV field, there still exists some drawbacks for clinical use of EVs as delivery systems, as there is no standardized, scalable, reproducible methods for EV isolation and EV loading of therapeutic cargos. EVs released by the cells may exert different responses in the receptor cells. The response of the EVs delivery indicate that EV may have different functions, which may depend on the donor cells or the EV markers, that depend on the pathway of formation of the EVs. This heterogeneity of EVs causes a big struggle in this study, as no knowledge has been obtained on which subpopulations may have an efficient RNA delivery[7,9,11,24,32].

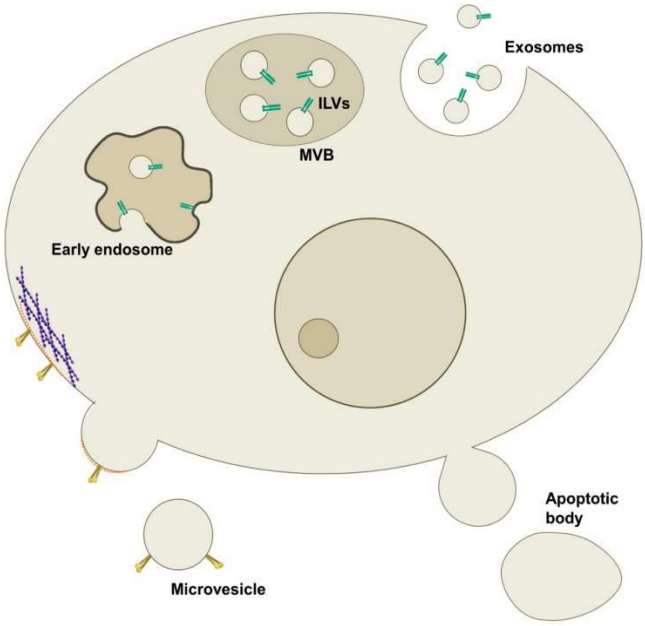


Figure 1.1. Different pathways of release of Extracellular vesicles. Schematic representation of different pathways of formation of different EV subtypes[33]

### 1.2.1 EV Markers and EV Functionality

To better understand EV functions in the body different proteomics analysis have been done over the years to clarify if the proteins present in the EV surface can indicate the EV function. However, the proteins on the surface differ depending on the EV subtype, pathway it was formed, type of donor cell and the functionality designated by the cell itself. As such, the community has disputed on what can be considered the EV markers[32–35]. For exosomes, proteins associated with its pathway of formation are mostly present in their surface as ESCRT associated or endosomal sorting complex or vesicular trafficking such as ALIX (Programmed cell death 6-interacting protein), CHMP4A-B, flotilin-1 and Caveolin-1. Others were associated with the sequestration of cytosolic proteins to the intraluminal vesicles such as heat shock protein 70 kDa (HSP70), heat shock cognate 70 kDa (HSC70) and beta-actin[33,35]. Some identified markers were considered to be present in small extracellular vesicles (sEVs), EVs that pass through a 220nm porous filter, which are usually considered exosomes in the literature[33,35,36]. However other EV populations may be present due to the lack of isolation techniques to obtain solely one population. Literature has presented specific markers that were only present in the sEVs such as Annexin XI, ADAM10, Syntenin 1 and TSG101[36–39]. The CD9, CD63, CD81 tetraspanins are also considered usual EV markers as they have been used multiple times for EV

immunoprecipitation and other techniques[34,40]. Other proteins associated with the extracellular matrix may also be present, in low quantities due to the pathway of formation of the vesicles, being the most commonly present fibronectin[34,36,37].

### 1.2.2 Tetraspanins and EV subpopulations

Tetraspanins are a big family of proteins with more than 30 different proteins, characterized by their common secondary structure. This family has been shown to be associated with different cellular processes such as adhesion, morphology, fusion and signaling, and are usually used as EV markers due to their high enrichment compared to the donor cells[27,41]. However, different studies have shown that tetraspanins such as CD9, CD63 and CD81 were present in different populations of EVs with different sizes. Nonetheless, tetraspanins have been shown to have a big role in the EV formation and cargo sorting, but no evidence in the CD9 and CD63 involvement in the EV-mediated RNA delivery[41–43]. As such, it is valuable to further understand how tetraspanins can influence the targeting and function of EVs, as they are currently being considered as EV subpopulations markers. CD9 and CD81 have been shown to be present in biogenesis of EVs by the plasma membrane while CD63 enriched EVs corresponded to endosome-derived EVs[36,43–45]. For isolation of the subpopulations immunoprecipitation is the most commonly used method. Use of antibodies for the targeting of the different tetraspanins allow a specific targeting to the subpopulations while maintaining the EVs intact. The capture of EV by targeting specific markers, increases the purity while targeting the EV subpopulations and maintains EV integrity, essential for their use in functionality experiments. Such approaches are usually done using a bead-based approach, a versatile method, with compatibility for experiments associated with Western Blot, qRT-PCR and flow cytometry. The most commonly used beads in immunoprecipitation protocols are latex beads, however this involved multiple centrifugation steps, and presents challenges in the reproducibility. As an alternative, a magnetic separation using magnetic beads has been developed for EV isolation, allowing the isolation of homogeneous population of EVs, both in size and morphology. Nonetheless, a small sample volume is necessary[36,37,46,47].

### 1.2.3 EV Isolation

One of the biggest issues for the use of EVs as therapeutic delivery systems has been the lack of standardized, scalable, reproducible and clinically-accepted method of EV isolation that would result in a considerable EV yield. The most common technique has been the ultracentrifugation as it is does not require expensive reagents and pre-treatment. However an ultracentrifugation machine is necessary. This technique relies on the sedimentation at high speed to separate EVs from other cellular components. Although, this is the most common technique,

it is time consuming and may cause reduced EV yields and low functionality results due to the damages caused by the force applied to the EVs in ultracentrifugation at high speed[40,46,48]. Other techniques commonly used are the density gradient, where a solution of sugars, like sucrose, is used to separate the sample per different densities. This technique is mostly used for EV purification allowing to remove contaminants such as fluorescence dyes or to separate EV subpopulations based on density. However different EV subtypes may possess the same density, rendering this technique unsuitable for the study of specific EV subpopulations functions[35,48]. Immunoprecipitation is also commonly used for proteomics analysis, as by targeting common EV markers, such as CD9, CD63, and CD81 allows to obtain a sample less contaminated by lipoproteins[48]. Other technique that has been emerging for EV isolation is the combination of ultrafiltration and size exclusion chromatography. This combination has been used since it is a faster technique, presenting similar yield comparing to the ultracentrifugation, while being additive-free and with similar purity[46,49]. The technique used should be carefully chosen depending on what it is desired to study as different techniques may present disadvantages and advantages to the study.

### 1.2.4 EV Loading

One of the biggest disadvantages in the use of EVs as therapeutic delivery systems has been the poor loading efficiency as only a small amount of EVs will present a therapeutic molecule[45,50]. Different methods have been developed for active loading of cargo into the EVs to improve the study of EVs. The most prevalent approach to enhance the active loading of cargo is endogenous loading, wherein cells are genetically engineered to express a recombinant protein serving as an anchor for cargo loading. For example, the expression of an eGFP protein fused with an EV marker demonstrated an increase in loading efficacy compared to the passive loading[45]. Another way is by exogenous loading, after isolating the EVs, the sample would be incubated with the therapeutic molecule and would bind on the surface[45,51]. This method is used when the cargos are small molecules that the cells does not have the machinery to manufacture, and the cargo stays on the outside of the EV. Loading of the cargo in EV is usually done by electroporation as it was already shown by the delivery of RNA, loaded by electroporation, to pancreatic ductal carcinoma in mice[51,52].

Another method for active loading involves transfecting of cells with protein anchors that can bind to the expressed active content enabling an efficient loading. However for efficient delivery it is also essential to ensure an efficient release of the active content from vesicles to reach the cell nucleus[45,51,52]. For efficient release, one possibility would be to use photocleavable linkers in the recombinant protein. This approach would enable complete release of the active

content by breaking the connection by UV-illuminating the EV samples before adding to the receptor cells[53].

## 1.3 Phosphatidylserine

The enrichment of extracellular vesicles with the negatively charged lipid phosphatidylserine (PS) has been consistently described. Lipids may have an important role in the EV function as they mediate EV endocytosis in immunocompetent cells. In addition to their known functions, research has demonstrated the presence of PS in the EV biogenesis. It has been observed that, under normal conditions, PS is predominantly situated in the inner leaflet of the cell membrane and asymmetrically maintained by flippase enzymes.During EV formation the asymmetry is lost and EV exposing PS are released[50,54,55]. The presence or enrichment of such lipids may then be related to different functions of the EVS such as the PS enriched EVs subpopulation may be of importance to remove cell waste. It has been demonstrated that the exposure of PS in a membrane surface is a classical "eat-me" signal for uptake by phagocytic cells. In the literature, it has been observed the existence of PS enriched EVs when compared to their donor cells[50,54,55]. This observation suggests the existence of an EV subpopulation enriched in PS, which may play a role in the disposal of cellular waste[54].

## 1.4 Vesicular Stomatitis Virus Glycoprotein

Vesicular stomatitis virus glycoprotein (VSV-G) is a protein expressed by virus in their surface in order to avoid endosomal degradation and escape to the intracellular space. The effect of VSV-G and other lentivirus proteins on EVs endosomal escape has been previously described[10,52,56,57]. It has been shown in different studies, that HEK293T EVs show a functional RNA delivery dependent of VSV-G[10,56,57]. Apart from the delivery VSV-G also increases the production of EVs by the cells[10,57].

## 1.5 EV Donor Cells

For the study of therapeutic delivery systems it is necessary to have donor cells to produce functional EVs used in the desired experiments. EVs can be isolated from in vitro cell cultures or directly from body fluid samples. Different donor EV cells are also important to analyze because EV function, cargo and biodistribution may depend on their donor cells and their biogenesis[27,58]. Cancer Cell lines and other immortal cell lines are typically chosen since they are easily cultured in vitro and with an efficient cell metabolism for a fast production of EVs[11,59]. Stem cells, as for Mesenchymal stem cells and cardiac progenitor cells (CPCs) can also

be used as donor cells as their EVs have been shown to present innate EV function when promoting angiogenesis, cell proliferation endothelial signaling and migration[23,28,60].

## 1.6 Study of EV-mediated RNA delivery

The investigation of EV-mediated RNA delivery has posed some challenges due to the absence of suitable analytical methods. Additionally, the study of RNA functionality has presented difficulties, particularly in distinguishing whether the cell-response is the result of the functional delivery of the RNA or the delivery of the transduced proteins[25]. It is essential for the reliability of the results that the methods enable the analysis of RNA delivery either directly or undirectly.

### 1.6.1 CROSS-FIRE System

The CRISPR Operated Stoplight System for Functional Intercellular RNA exchange (CROSS-FIRE) system was a system designed by Dr. Olivier G. de Jong to analyze the transfer of EV-mediated RNA by utilizing CRISPR/Cas9 gene editing technique [25].. For this method a fluorescent "Stoplight" reporter system is permanently activated in EV-acceptor cells upon functional EV delivery of sgRNA, expressed in donor cells . The reporter system cells used in the CROSS-FIRE system are modified to permanently express mCherry, followed by a "linker" region between the mCherry and its stop codon. Upon delivery of functional sgRNA and Cas9, the linker is recognized by the complex sgRNA and Cas9, and creates a double stranded break in the DNA resulting in a frameshift of 1 or more nucleotides (Figure 1.2.). The stop codon is then bypassed and the cells will permanently express eGFP. This system has been seen as a highly sensitive method to study EV mediated RNA delivery to a single cell resolution[25].

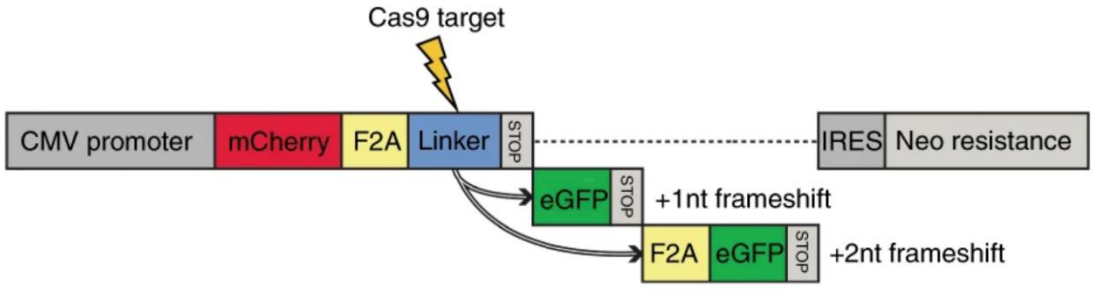


Figure 1.2. Schematic of the stoplight reporter system permantly expressing mCherry under a CMV promoter, followed the Cas9 targeted linker region and a stop codon. Two eGFP open reading frames one or two nucleotides out of frame. When a frameshift was caused by a Cas9-mediated cut in the linker region, one of the eGFP reading

frames will be expressed simultaneously with mCherry. Self-cleaving F2A peptide domains are placed between the fluorescent proteins[25].

### 1.6.2 Wound Healing Assay

Cardiac Progenitor cells (CPCs) EVs have previously been documented to stimulate signaling and migration of endothelial cells. These EVs facilitate the migration of endothelial cells through proteins contained within them, which activate cellular migration mechanisms. This particular function has been utilized in the assessment of EV functionality. By introducing CPC EVs to endothelial cells and analyzing the migration researches can investigate the role and functionality of these EVs and their subpopulations[60,61].

## 1.7 Objective

The objective for this project was to compare the RNA delivery efficacy of different extracellular vesicles subpopulations using the CROSS-FIRE system. By transfecting donor cells to express VSV-G, Cas9, sgRNA, and a designed anchor, the EVs and the subpopulations would be isolated and transferred to reporter cells to analyze the reporter cell activation. An extra experiment done was the use of CPC EVs, and addition to endothelial cells to further confirm if any EV subpopulation presented an increased in cell migration. If any subpopulation presented an increased delivery efficacy, it would promote a further development of delivery systems using the specific subpopulation.

EN: “The research work described in this dissertation was carried out in accordance with the norms established in the ethics code of Universidade Nova de Lisboa. The work described and the material presented in this dissertation, with the exceptions clearly stated, constitute original work carried outby the author.”

PT: “O trabalho de investigação descrito nesta dissertação foi realizado de acordo com as normas estabelecidas no código de ética da Universidade Nova de Lisboa. O trabalho descrito e o material apresentado nesta dissertação, com as exceções claramente indicadas, constituem trabalho original realizado pelo/a autor/a. “

# 2 MATERIALS AND METHODS

## 2.1 Cell Culture And EV production

HEK293T and HeLa cells were cultured in T175 flasks using Dulbecco's Modified Eagle Medium (DMEM, Gibco), supplemented with 10% heat-inactivated Fetal Calf Serum (FCS) and 1% penicillin and streptomycin (P/S). Trypsin/EDTA (1%) in PBS (Sigma) was used to create a single cell suspension and splitting cells. When the cells presented a confluency of 70-80% they were washed with PBS and cultured in Opti-MEM (Gibco) supplemented with 1% P/S, for at least 16 hours before EV isolation.HEK293T Stoplight cells without Cas9 expression, kindly given by Dr. Olivier Jong [25]., were cultured in DMEM supplemented with 10% FCS, 1% P/S, and 1mg/mL G418. Cardiac Progenitor Cells (CPCs) were cultured in CMPC:SP++ medium, which consisted of 22% fully supplemented EGM-2 medium (Lonza), 66% M199 (Gibco), 10% FCS, 1.1% MEM-NEAA (Gibco) and 0.9% P/S, on flasks coated with 0.1% gelatin in PBS. For CPC EV production the cell surface was washed with PBS and the culture medium was replaced for M199 (Gibco). HMEC-1-eGFP cells were cultured in MCDB 131 (Gibco) supplemented with 10% FCS, 1% P/S, 0.5mg/mL G418, 1ng/mL human Epidermal growth factor (hEGF, Sigma), 50nM hydrocortisone (Sigma) and 1% L-Glutamine (Peprotech) on surface coated with 0.1% gelatin. All the cells were incubated at 37ºC and 5% CO2.

Transfection was done when the cells presented a 40% confluency for EV production. For the transfection 40µL of Polyethylenimine (PEI) was added to the desired amount of Opti-Mem (Gibco) and incubated for 5 minutes. Plasmids encoding for VSV-G, Cas9, sgRNA with MS2 aptamers and the desired recombinant protein encoding plasmid associated with a photocleavable domain and a human influenza hemagglutinin (HA) tag (CD9-PhoCl-MS2, Myr-PhoCl-MS2, CD81-PhoCl-MS2) (Kindly offered Dr. Olivier Jong, manuscript in progress) were used (Figure 2.1). A total of 20µg, 5µg of each plasmid per flask was added to the desire amount of Opti-Mem and mixed with the PEI solution.

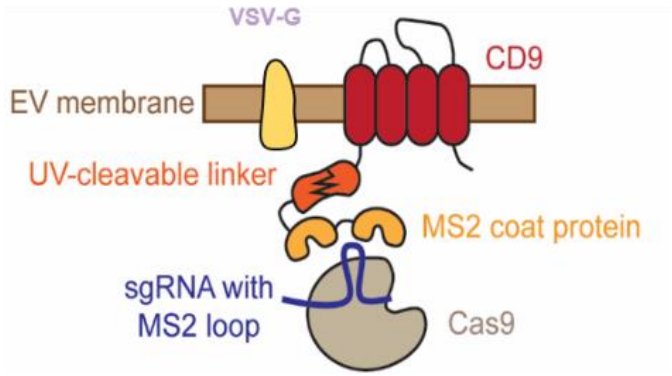


Figure 2.1. Schematic of the EV membrane when expressing VSV-G, recombinant protein anchor formed with a CD9 tetraspanin, a UV-cleavable linker and a MS2 binding domain, binding to the sgRNA with a MS2 loop and the Cas9.

## 2.2 EV Isolation

The EV production medium was collected after the cells incubated for 16 hours in the medium. After collection, to remove cell debris, the sample was spun down at 300g before being transferred to a new tube and centrifuged at 2000g for 10 minutes at 4°C. The supernatant was filtered through a 0.45µm Rapid Flow Filter (Nalgene). A tangential flow filtration Minimate™ capsule (100K molecular weight cut-off (MWCO)), was used to concentrate the filter flow through to approximately 30mL .PBS was used to wash the system and added to the sample. Further concentration was done using an 100kDa MWCo Amicon® Ultra-15 centrifugal filters (Merck Milipore), pre-flushed with PBS at 3000g for 5 minutes.

## 2.3 Size Exclusion Chromatography

To remove unbound protein, size exclusion chromatography was performed with a HiPrep 16/60 Sephacryl S-400 HR column (GE Healthcare) packed with Sepharose 4 Fast Flow-packed resin that was calibrated with PBS and connected to a refrigerated ÄKTA Start system.The flow rate was changed to 0.5mL/min before injecting the sample. The EV fractions were identified and collected according to the UV absorbance. The fractions total volume of 4mL was further concentrated to approximately 250µL using 100kDa MWCo Amicon® Ultra-4 centrifugal filters (Merck Milipore), pre-flushed with PBS at 3000g for 5 minutes.

## 2.4 Memglow Staining

In order to perform a fluorescence-based normalization, the EV samples that were on experiments involving the CROSS-FIRE system were stained with MemGlow. The EV sample was previous concentrated to a volume below 250 µL as described above
MemGlowTM 590 (200 µM in dimethyl sulfoxide (DMSO, Cytoskeleton, Inc.)) was diluted in PBS in a ratio of 1:50 and a total volume equal to the volume of the samples. The solution was then added to the sample, having a total dilution ratio of 1:100, and incubated for 30 minutes. Afterwards, size exclusion chromatography was performed in a XK-16/20 column (GE Healthcare) packed with CL-4B resin with the same procedure as described above.

## 2.5 Nanoparticle Tracking Analysis (NTA)

After concentrating EV samples, the particle concentration of the EV samples was measured using the NanoSight S500 system (Malvern Panalytical). The EV samples were diluted in PBS to achieve the desired concentrations for the analysis. PBS was analyzed as a blank sample. The sample were analyzed in five 30s movies with a camera level of 15 at 25ºC. The data was analyzed by NTA 3.0 software with the detection threshold set at 7.

## 2.6 EV Subpopulation Isolation

The particle concentration, previously obtained by NTA, was used in order to calculate the necessary amount of EV, antibodies and PBS (Sigma) for each subpopulation pulldown (Table 1.). As an example, consider the particle concentration to be 5.00E+10 particles per pulldown, incubated with 8.33µL of magnetic beads (Dynabeads™ Protein G, Invitrogen) per pulldown (Table 2.). The EV sample was divided into 5 Eppendorf's, the EV samples for the isolation of CD9+, CD63+ and CD81+ subpopulations were incubated with their respective antibodies for 30 minutes at room temperature (RT). The phosphatidylserine (PS) subpopulation was first incubated with R2-C1C2, which binds to PS (50) for 15 minutes and then incubated with the Anti-Myc, which binds R2-C1C2, for another 15 minutes. Magnetic beads (Dynabeads™ Protein G, Invitrogen) were washed with 300µL 5 times with PBS 0.001% v/v Tween20 (PBS-T), before being divided into 4 eppendorfs. Before adding the samples to the beads 10% of the volume was transferred to another eppendorf and used as antibody control. The EV stock, sample used as control and not treated with any antibodies, was diluted in the same ratio as the subpopulations. All samples were vortexed, centrifuged and left in the rotator overnight at 4ºC to keep all the conditions equal. The next day, with the magnetic rack, the supernatant of each pulldown was removed to another eppendorf and stored on ice. The beads were

washed 5 times using PBS-T. The elution was done using the Sodium Hydrogen Orthophosphate Buffered Saline buffer (SHOBS) (0,85% NaCl, 50mM Na2HPO4, 12.5mM NaOH) pH 11.20 with the desired incubation time between 1 to 5 minutes. After the desired incubation time the sample was spun down and the eppendorf put back in the magnetic rack. The sample was removed from the eppendorf and added to a new one which contained the Neutralization Buffer (1M Tris-HCl) with a pH 3.90 in a sample: Neutralization buffer ratio of 1:0.15. The Antibody control samples were also treated with the respective SHOBS Buffer volume and afterwards neutralized in the same ratio as the other samples to obtain the same volume in all samples. EV Stock sample was then diluted to a ratio of 1:20. 10 µL of the samples and the dilluted EV Stock was pippeted to a black 384-well plate to measure fluorescence using the SpectraMax® iD3 (Molecular Devices) at 573nm for excitation and 613nm for emission.

Table 2.1. Antibodies used for subpopulation Isolation

**Pulldown antibodies**

| **Target** | **Species** | **Manufacturer** | **Catalog#** | **Clone** | **Ab system #** |
|---|---|---|---|---|---|
| CD9 | Mouse | Sigma | CBL162 | MM2/57 | 808 |
| CD63 | Mouse | Abcam | ab8219 | MEM-259 | 2240 |
| CD81 | Mouse | Diaclone | DC-857.780 | TS81 | 811 |
| Anti-Myc | Mouse | Home-made | | 9E10 | 2377 |

Table 2.2. Example of a EV subpopulation isolation

| **Capture Antibody** | **Amount of antibody to add (µg)** | **Amount of EVs added (particles)** | **Amount of Magnetic beads used (µg)** |
|---|---|---|---|
| Anti-CD9 | 0.15 | 0 | 0 |
| Anti-CD63 | 1.5 | 0 | 0 |
| Anti-CD81 | 0.2 | 0 | 0 |
| R2-C1C2 | 0.84 | 0 | 0 |
| Anti-Myc | 1 | 0 | 0 |
| EVs per pulldown | 0 | **5.00E+10** | 0 |
| Magnetic beads | 0 | 0 | **8.33** |

## 2.7 Western Blot

In order to proceed with the Western Blot, 3x Laemmli sample buffer (House made, CDL UMCU, Utrecht, The Netherlands) was added to all samples in a ratio for it to be diluted to 1x

Laemmli sample buffer. The samples were divided over two PCR tubes, to create non-reduced and reduced samples, by addition of dithiothreitol (DTT). All samples are incubated at 95ºC for 10 minutes while pre-made gels (BoltTM 4-12% Bis-Tris-plus, Invitrogen) was prepared. All samples, and protein marker (Precision™ Plus Protein Standard, Bio-rad) were added into the wells. The gel was run for 45 minutes at 165mV in a container filled with 1x MOPS running buffer. Afterwards, the samples were transferred to a polyvinylidene fluoride (PVDF) membrane in blotting buffer (25mM Tris, 192mM Glycine, 20% v/v ethanol) at 125mV for 65min in a tray with ice. The membrane was blocked for at least 120 min with a solution made from 50% v/v Tris buffered saline (TBS) and 50% v/v Intercept® blocking buffer (LI-COR). Primary and secondary antibodies were added to a 50% v/v TBS with 0.1%v/v Tween 20 (TBS-T) and 50% v/v Intercept® blocking buffer and incubated for 2 hours at RT or overnight at 4ºC and 45 minutes at RT for the secondary antibody. All antibodies used are listed in Table 2. All blots were scanned on the Odyssey M imager (LI-COR) at 700 and 800nm.

Table 2.3. Primary and Secondary antibodies used for Western Blot.

**Primary antibodies**

| Target | Species | Target size (kD) | Dilution | Manufacturer | Catalog# | Clone | Ab system # |
|---|---|---|---|---|---|---|---|
| Alix | Mouse | 96 | 1000 | Thermo Scientific | MA1-83977 | 3A9 | 2220 |
| Annexin A1 | Rabbit | 39 | 1000 | Abcam | ab214486 | EPR19342 | 2504 |
| Beta-actin | Mouse | 45 | 1000 | Cell Signaling | #3700 | 8H10D10 | 2221 |
| Caveolin-1 | Rabbit | 20 | 2000 | Abcam | ab192869 | EPR15554 | 2327 |
| CD63 | Mouse | 25-70 | 1000 | Abcam | ab8219 | MEM-259 | 2240 |
| CD81 | Mouse | 25 | 1000 | Santa Cruz | sc-166029 | B-11 | 806 |
| CD9 | Mouse | 25 | 1000 | Sigma | CBL162 | MM2/57 | 808 |
| Fibronectin | Rabbit | 220 | 1000 | Sigma | F3648 | | Cardio -20°C |
| Flotillin-1 | Rabbit | 47 | 1000 | Merck Milipore | MABN1118 | EPR6041 | 2316 |
| HA-tag | Rabbit | 50 | 1000 | GeneTex | GTX115044 | | 2436 |
| VSV-G | Mouse | 50 | 1000 | | | 8G5F11 | |
| Syntenin | Mouse | 33 | 500 | Origene | TA504796 | OTI2H6 | 2444 |
| TSG101 | Rabbit | 45 | 1000 | Abcam | ab30871 | ERP7130(B) | 2239 |

**Secondary antibodies**

| Target | Species | Conjugate | Dilution | Manufacturer | Catalog# | Clone | Ab system # |
|---|---|---|---|---|---|---|---|
| IgG Mouse | Goat | Alexa 680 | 7500 | Life/LI-COR | A21057 | | 712 |
| IgG Rabbit | Goat | Alexa 680 | 7500 | Life/LI-COR | A21076 | | 714 |
| IgG Mouse | Donkey | IRDye 800CW | 7500 | Odyssey | 926-32212 | | 2278 |
| IgG Rabbit | Goat | IRDye 800CW | 7500 | Odyssey | 926-32211/B81009-02 | | 2280 |

## 2.8 Flow Cytometry Analysis of Magnetic Beads used in EV Subpopulation Isolation

Magnetic beads were analyzed by flow cytometry after subpopulation isolation in order to verify if the VSV-G had any effect on capture and elution of the EVs out of the magnetic beads. Before elution, 6 µL of all of the bead samples previously incubated as stated in the section 2.6, and were collected to a new eppendorf as the "pre-elution" sample. After elution with the SHOBS Buffer and the neutralization buffer in the respective ratio mentioned above, the beads were diluted in PBS-T 0.001% and added to new eppendorfs as "pos-elution" sample to analyze the amount of EV still attached to the beads. Empty beads were used as a black control by adding 0.1 µL of washed empty beads to each well as negative control. The 2 µL of the bead samples were added in triplicate to a U-bottom 96 well plate with 100µL of PBS. The plate hence contained pre-elution, pro-elution and negative control beads. To remove the supernatant out of the wells, the plate was placed on top of a magnet and the liquid was slapped out of the wells to the sink. The beads were then mixed with a staining solution of PKH67 dye and Diluent C (Sigma MIDI67-1KT) in a ratio of 1:550 respectively, and incubated 5 minutes at RT. PKH67 is a lipidic dye that is incorporated in the membrane thus staining the EVs. The beads were washed with 150 µL of PBSA (PBS with 1% Bovine Serum Albumin), this procedure was repeated 3 times. After removing the wash, the beads were once again ressuspended in 200µL PBS-T 0.001%. Fluorescence measurement and analysis was done in FACSCanto II flow cytometer (BD Biosciences) and BD FACSDIVA software.

## 2.9 Evaluation of the Elution Incubation Time by Flow Cytometry

To evaluate how the incubation time affected the EV samples elution, 1.05 µL of beads were previously incubated with the EV samples as stated in the EV subpopulation isolation section 2.6. After incubation with the EV samples, all magnetic bead samples were divided into 7 new eppendorfs. The PBS-T was removed and 100µL of SHOBS buffer were added and incubated for 0, 1, 2, 3, 4, or 5 minutes. After incubation the buffer was removed, 60µL of PBS-T was added, and the samples were divided over 3 well of a U-Bottom 96 well plate, previously filled with 100µL PBS-T on each well. As controls, 0.5 µL of washed empty beads were transferred to the respective triplicate negative control wells. Afterwards dyeing of bead samples was done as stated above in section 2.8.

## 2.10 CRISPR-Cas9-Based Reporter System

To investigate the RNA delivery efficiency of the different EV subpopulation the CROSS-FIRE reporter system was used. For this method, cells were transfected and EVs and the EV subpopulations were isolated according to the method described above. One day before the addition of the samples to the reporter system, the reporter cells (HEK293T Stoplight, Olivier de Jong) cells were plated in a 48-well plate at 26.000 cells per well in 0,5mL medium or in a 96-well plate at a 8.600 cells per well in 0.1 mL. The Stoplight cells constitutively express mCherry. When the cells receive the Cas9 sgRNA complex, it causes a frameshift starting the permanent co-expression of eGFP by the cells (Figure 1.2). The samples were normalized based on fluorescence in Spectramax ID3 (Molecular Devices), and diluted accordingly. The samples were illuminated for 20 minutes by UV-light (400nm) on ice. Afterwards the sample was added to the cells in triplicate and incubated for four days. After adding the samples, as positive control, cells were transfected with 125ng of the plasmids encoding for Cas9 and the sgRNA with MS2 aptamers with 0.5 µL of PEI in 50 µL per well according to the procedure described in section 2.1. As a negative control, the SHOBS buffer was mixed with the neutralization buffer in the SHOBS: Neutralization ratio of 1:0.15. The wells were imaged after the four days incubation, using an EVOS M5000 Imaging System (Thermo Fisher Scientific). All pictures were taken with a 10x magnification with brightfield, GFP and RFP filters. For flow cytometry analysis, the medium was removed from the wells and 100µL of TE were used to form a single cells suspension. After detachment of the cells, suspension was transferred to a new U-Bottom 96 well plate previously filled with 100µL of the growth medium for inactivation of the trypsin. The cells were pelleted at 300g for 5 minutes. The medium was then aspirated carefully to not aspirate the cell cluster and ressuspended in FACS buffer (0.3% BSA in PBS). Quantities of mCherry and eGFP-positive cells were determined on FACSCanto II flow cytometer (BD Bioscience) and analyzed in BD FACSDIVA software. The percentage of eGFP-positive cells was obtained by dividing the eGFP cell count by the mCherry positive cells and multiplying by 100.

## 2.11 Wound Healing Assay

To analyze EV subpopulation uptake CPC EVs and subpopulation were previously isolated as described above. 24 hours prior to the assay, HMEC-1-eGFP cells (Stably transduced and kindly provided by Dr. Olivier de Jong) were seeded in a 96-well plate at a density of 40.000 cells per well. On the next day, wounds were made from top to bottom in all wells, by scratching the surface with a sterile p200-pippete tip. The wells were washed 2 times with PBS, and

then 100µL of MCDB 131 supplemented with 1% P/S was added to the wells. Fully supplemented MCDB 131 was added to the cells in triplicate for the positive control. After the EV samples were added to the cells in triplicate, imaging was conducted, using an EVOS M5000 Imaging System (Thermo Fisher Scientific) at 40x magnification with the green fluorescence filter. Photos were taken after adding the samples, considering t1=0 hours, the moment of the first photo, and a second photo capture done after 6 hours (t2). To make sure the images presented the same filed of view, the corners of the wells were used as reference. Two pictures were taken per well one at each end of the scratch. Wound area was analyzed with a wound healing size tool plugin of ImageJ. Variance window radius was set at 20. Threshold value was adjusted according to previous results from previous students. For t1 images threshold was set at 80. For t2 threshold was set at 40. The same settings were used for all the pictures taken. The effect of the EVs was calculated by the wound closure area and the regrowth percentage (Figure 2.2).

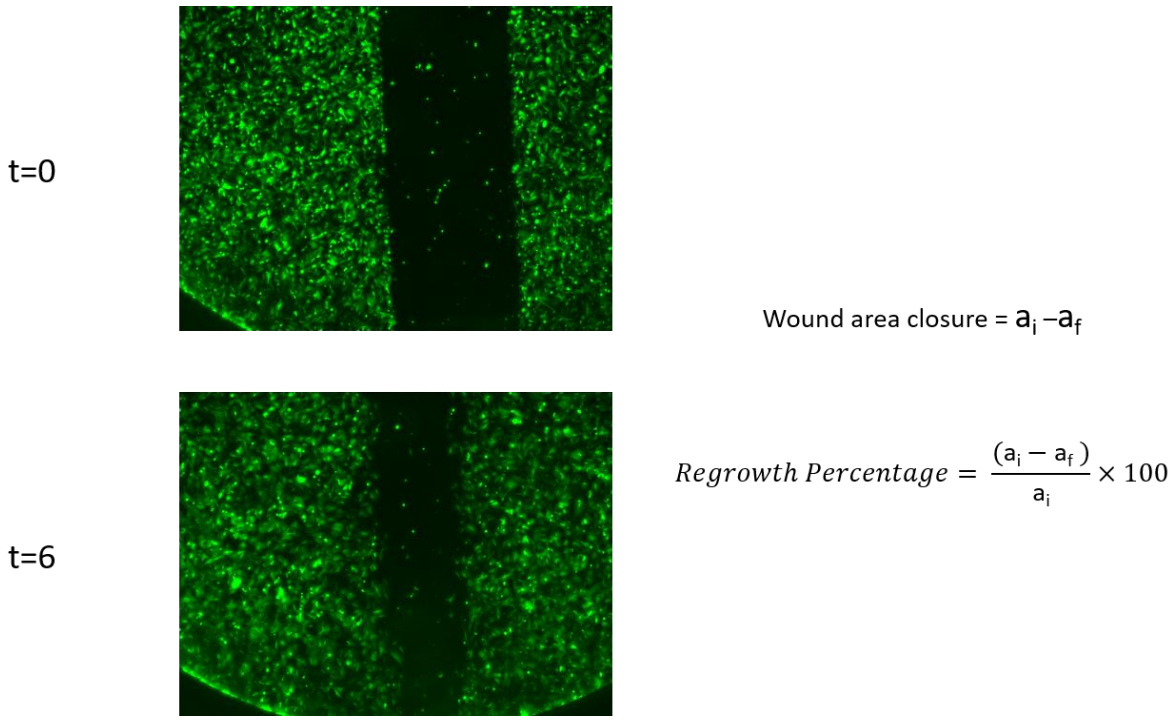


Figure 2.2Calculation of wound closure area and regrowth percentage for assessing the effect of the EVs on the HMEC-1 eGFP regrowth. Where $a_i$ corresponds to the area of pixels at t = 0 and $a_f$ the area of the pixel at t = 6 hours.

# 3 RESULTS

## 3.1 CD81 enriched EVs show higher system activation of CD9+ subpopulation

Sander and previous students on the project developed a stable elution buffer that would elute the subpopulations with the minimum amount of damage to their functionality. CD81 was overexpressed in the cells as a fusion construct with MS2-binding domains (Referred as an EV-anchor) and used in this first experiment since no previous data was obtained using this construct in combination with the new buffer developed. The EVs and their subpopulations were isolated from transfected HEK293T cells as described in section 2.2 and 2.6, respectively.EV subpopulations were added to the cells after normalizing based on fluorescence. The MS2-binding domain on the engineered CD81 anchor expressed allows for the binding with MS2 aptamers on the RNA and thus for an efficient loading. Further on the sample was UV-illuminated in order to destroy a photocleavable domain present in the anchor. Destroying the linker separated the CD81 tetraspanin from the MS2-binding domain which bound the anchor and the sgRNA. The reporter cells would co-express mCherry and eGFP when the photocleavable domain present in the EVs was destroyed, allowing for an efficient release of the sgRNA and Cas9 which would remove the linker sequence, causing a frameshift which would enable the expression of eGFP. When a CD81-PhoCl-MS2 anchor was used (Figure 3.1.) the CD9+ subpopulation showed the highest activation of the subpopulations, followed by the CD81+ subpopulation. CD63+ and PS+ subpopulations did not present a relevant activation of the system, showing values in the same order as the negative control. The maximum activation of the system was observed in the EV stock, which is the initial sample that contains all of the subpopulations. The stock was used as a positive control for the maximum activation value. Through observation of the EV stock, the activation of the system was observed to be dose-dependent. The sum of the high dose of any subpopulation and the respective supernatant should equal the maximum activation presented equal to the activation on the EV stock at the highest dose. The CD63+ supernatant sample showed a system activation similar to the EV stock at the highest dose, presenting a low to no activation of the system in any other dose sample of the CD63+ subpopulation. The PS+ subpopulation also does not present any activation for the isolated doses, showing only activation by the supernatant of the pulldown, which is the sample obtained after isolation of the PS+ subpopulation.

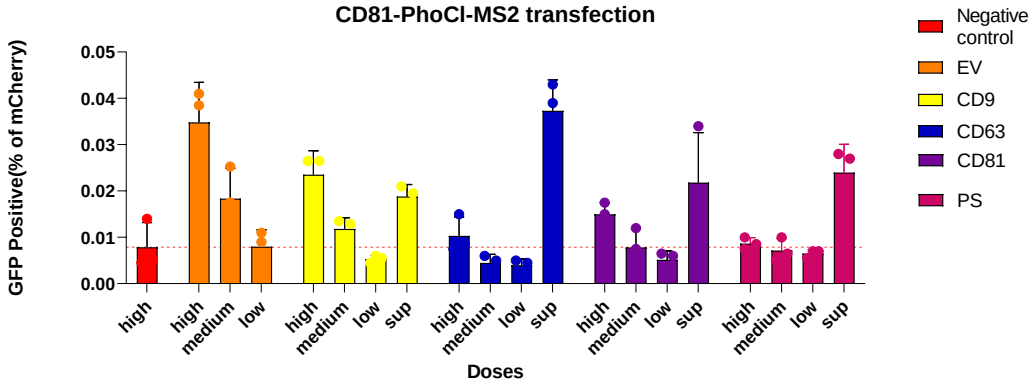


Figure 3.1. CD81 enriched EVs present higher activation of the CD9+ subpopulation. The functionality of EV subpopulations derived from HEK293T cells transfected with plasmids encoding for VSV-G, Cas9, sgRNA with MS2 aptamers and CD81-PhoCl-MS2 added in three doses (low= 629.21, medium=1258.43, high=2516.86 Memglow590-derived fluorescence) to HEK293T stoplight cells was analyzed by eGFP expression by flow cytometry 3 days after addition of the samples. EV stock sample, where no subpopulation was isolated and supernatants (sup), remnant of the subpopulation isolation were also added to the cells at the same particle yield.

## 3.2 Myr Enriched EVs are not efficiently isolated in the EV subpopulations

In order to avoid using an EV marker that we would capture in the subpopulation isolation for EV loading, a Myristoylation anchor was used. The use of the Myr anchor would allow an equal distribution of the active content through the subpopulation. To test the functional cargo delivery capacity it would be preferable the use of an anchor which would not be targeted for capturing, and that could cause the specifically loading of the cargo into one of the subpopulation that we are isolating. EV and subpopulation isolation was done as described in section 2.2 and 2.6 respectively, with the only difference being the transfected EV anchor used in this experiment. When the samples were added to the cells the EV subpopulations showed little to no activation of the system. Values around the negative control and below the lowest dose of the EV Stock showed a 90% activity loss when comparing it to the EV stock at the high dose (Figure 3.2.). The supernatant of all the subpopulations showed the maximum possible activation, equal to the activation of the highest EV Stock dose. These results indicate that we were not able to efficiently isolate our transfected EVs. The medium dose of the PS+ subpopulation in Figure 3.2.a shows a higher value compared to other samples. This could be caused due to technical errors or an artifact since only one value out of the triplicates exhibited a high activation.

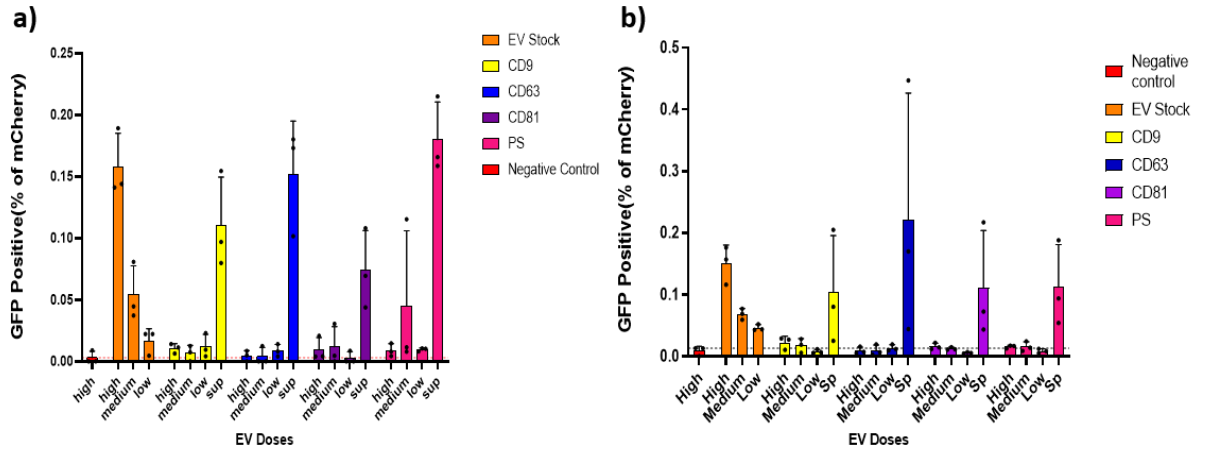


Figure 3.2. Myr enriched EV subpopulations did not present activation of the system .The functionality of EV subpopulations derived from HEK293T cells transfected with plasmids encoding for VSV-G, Cas9, sgRNA with MS2 aptamers and Myr-PhoCl-MS2 was compared in three different doses of Memglow590-derived fluorescence by the expression of eGFP by HEK293T Stoplight cells three days after the addition of the samples by flow cytometry. a)Low = 1442.28, medium = 2884.57, high = 5769.14 Memglow590-derived fluorescence b) Low = 3465.08, medium = 6930.17, high = 13860.33 Memglow590-derived fluorescence. EV stock sample, where no subpopulation was isolated and supernatants (sup), remnant of the subpopulation isolation were also added to the cells at the same particle yield.

To understand the efficiency of the pulldown, cells were transfected with the same plasmids. The transfected EVs were analyzed by western blot (Figure 3.3.) after isolation of the EVs and subpopulations accordingly. The membranes were stained using anti-actin, anti-TSG101, anti-Alix and anti-Syntenin. These antibodies are specific for proteins involved in vesicle biogenesis and therefore present on EVs, which allows their use as EV markers[38,39,62]. As shown on the Western blot, most of the EV markers were present in all samples, both pulldown (PD) and supernatant (SP). However, the EV marker bands appear to be more prevalent on the SP samples with the exception of Alix, which was mostly present on the PD. The fibronectin is an extracellular matrix protein that can be found on the surface of the vesicles. The results suggest that in the isolation process of the subpopulations, the fibronectin is removed from the surface causing it to only be present on the supernatant. Analyzing the CD9 and CD81 bands, we observe that the tetraspanins are mostly present in the pulldown samples. The CD81 band shows complete isolation on the CD81+ and CD9+ subpopulations especially for the CD9+ subpopulation. This may have been due to the presence of antibody remnants of the subpopulation isolation since the staining was done in reduced samples. The CD9 band shows that it was not completely isolated on the CD9+ subpopulation since a band is still present in the supernatant of the same subpopulation. The EV subpopulation isolation was highly efficient, however the HA-Tag was seen in both PD and SP samples which would suggest that our Myr

transfected EVs were not isolated in our EV subpopulations. Anti-VSV-G antibodies were additionally used for the western blot. This viral protein is highly expressed in the sample showing the efficiency of the cell transfection.

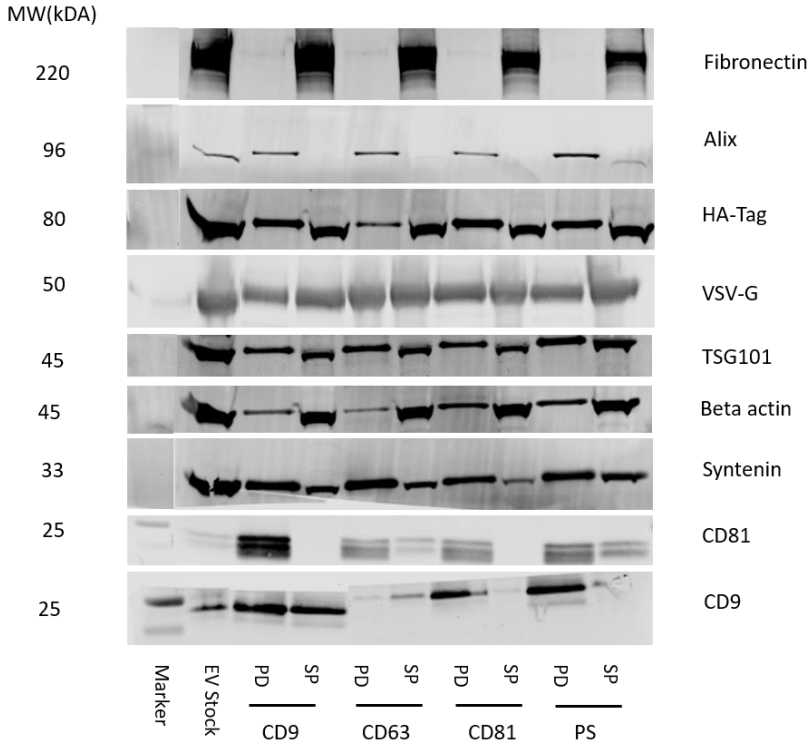


Figure 3.3. Western blot analysis of CD9+, CD63+, CD81+ and PS+ subpopulations isolation of Myr enriched EVs. Myr enriched EVs used for the subpopulation isolation are incubated with the targeting antibodies for each subpopulation and magnetic beads. Supernatant (SP) and pulldown sample (PD) are obtained and loaded in the same volume. EV markers such as Alix, TSG101, Beta actin, Syntenin, VSV-G and fibronectin are stained along with CD9 and CD81 tetraspanins considered as markers of the EV subpopulation. HA-Tag incorporated in the Myr-PhoCl-MS2 that was transfected are also stained.

## 3.3 Capture and elution of the EV subpopulations is affected by VSV-G expression

In order to analyze if the expression of VSV-G could be affecting the isolation of the transfected EVs, the magnetic beads were analyzed by flow cytometry. After transfecting two groups of cells with and without VSV-G, EVs were isolated according to the methods above. The used samples were normalized by NTA to have the same particle concentration before isolation of the subpopulations. The subpopulation isolation was done following the methods and with the same amount of magnetic beads and antibody for all samples. In the obtained results (Figure 3.4.), we can understand that all subpopulations with VSV-G show a lower capture of EVs. A lower capture resulted in a lower absolute value on the elution. The EVs without expression

of VSV-G showed a higher capture comparing to the EV samples expressing VSV-G, suggesting that if we could remove VSV-G out of the experiment formulation we could obtain a higher yield of EVs.

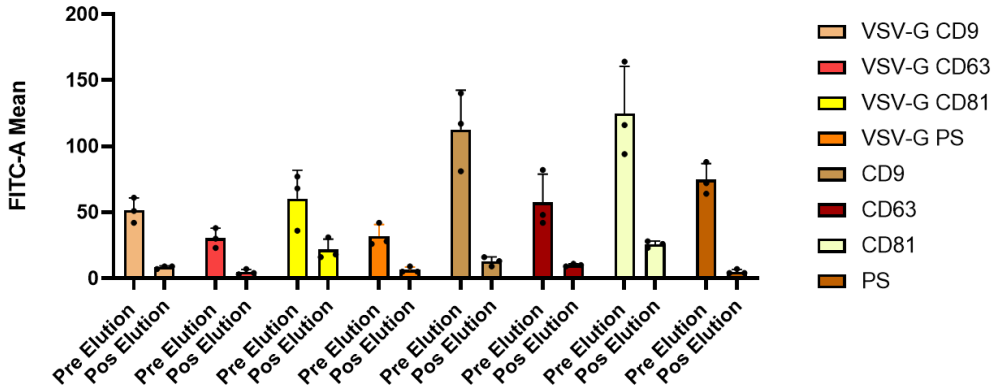


Figure 3.4. VSV-G affects the capture efficacy of the EV subpopulations. Samples pre-elution and pos-elution were taken of each subpopulation. EVs that remained in the magnetic beads were dyed with PKH67 and analyzed by flow cytometry.

## 3.4 HeLa EVs do not activate the CROSS-FIRE System without VSV-G Expression

In order to test if we could circumvent the use of VSV-G with a different cell line as EV donor, HeLa cells were transfected with and without VSV-G. This way the efficacy of activation of the CROSS-FIRE system could be analyzed without VSV-G expression in the EVs. In the executed experiment, the EV subpopulations were not isolated, so only serial dilutions with different EV particle concentrations were performed. For figure 3.5.a. cells were transfected with the encoding plasmids for Cas9, sgRNA and the myristoylation anchor with no VSV-G expression. The doses for this experiment were prepared in order for dose one to be the highest and 5 the lowest. None of the used doses showed an activation above background, with the exception of the SHOBS treated dose. However the discrepancy between values of the triplicate addition lead us to disregard this sample since it presented a particle concentration of 2.52E+09. It was considered to be an artifact since it exhibited a higher activation than doses with a higher concentration taking the expected functionality damage from the elution buffer into consideration. When the cells were transfected with plasmids encoding for VSV-G (Figure 3.5.b.) we can see a dose-dependent activation of the system. The highest dose showed around the same activation as the positive control, which was transfected with plasmids encoding for Cas9 and sgRNA. The lower the particle concentration of the sample, the lower the activation of the reporter cells observed. The SHOBS treated sample showed the lowest activation out of all

doses, although the particle concentration of this sample was higher than dose 2, it was not able to reach the same values of activation.

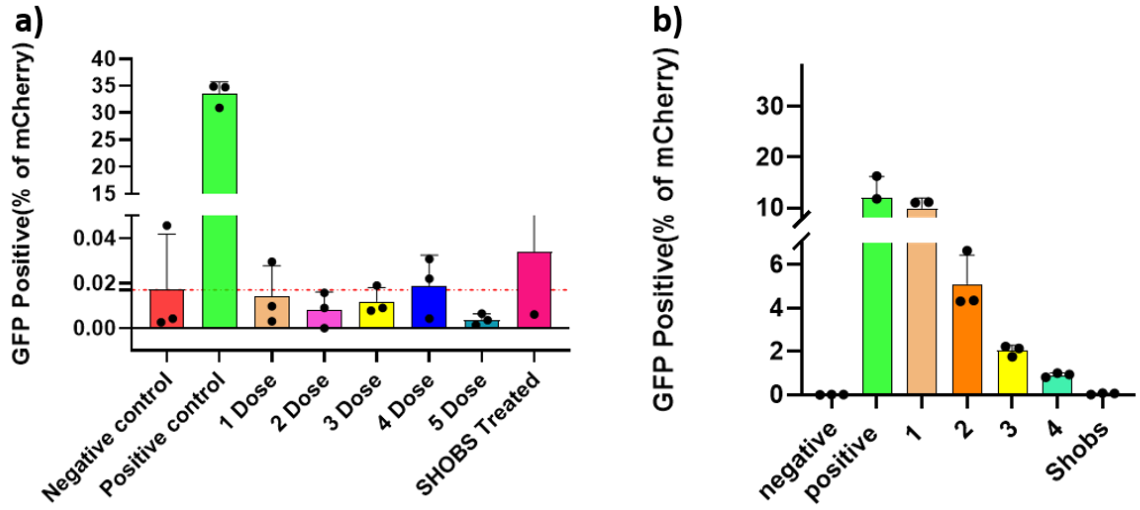


Figure 3.5. Myr enriched EVs from HeLa donor cells did not functionally delivered RNA without VSV-G. a) Engineered EVs transfected with plasmids encoding for sgRNA-MS2 aptamers, Cas9, Myr-PhoCl-MS2 were added to the reporter cells in serial doses (1 dose = 1.36E+10, 2 dose = 6.81E+9, 3 dose = 3.41E+9, 4 dose = 1.70E+9, 5 dose = 8.52E+8, SHOBS treated dose = 7.52E+9 particles per well) and measured by flow cytometry. b) Engineered EVs that were also transfected with plasmids encoding for sgRNA-MS2 aptamers, Cas9, Myr-PhoCl-MS2 and VSV-G were added to the reporter cells in serial doses ( 1 dose = 6.88E+10, 2 dose = 3.44E+10, 3 dose = 1.72E+10, 4 dose = 8.59E+9, SHOBS treated dose = 1.72E+10 particles per well) and measured by flow cytometry. Positive control was done by direct expression of sgRNA and Cas9 on the HEK Stoplight.

## 3.5 The functionality of the extracellular vesicles was pH-dependent

Previous results showed that it was necessary to express VSV-G on the EVs for a functional cargo delivery. Therefore we tried to understand where the protocol could be further optimized to improve the EV cargo delivery. To understand how the functionality of the EVs was affected by the elution buffer, the EV samples were eluted with SHOBS buffer in pH range 11.00-11.51. Other elution buffers from literature were also tested. To test if the antibodies could affect the functionality of the EVs samples, an incubation with the antibodies used in the subpopulation isolation was also done. For negative control, a non-illuminated EV sample was also done. After elution, the EV samples were added to the reporter cells and incubated 4 days before analysis (Figure 3.6.). The antibody controls showed similar activation of the system compared to the EV sample that was only UV-illuminated and not treated with any elution buffer. As explained previously the sample needs to be UV-illuminated for the content to be released out of the EVs to the cytoplasm. This can be seen from the unilluminated sample, which shows a loss of 90% of activation in comparison to the UV-illuminated sample. The

effect of the SHOBS buffer on the functionality was analyzed in a pH range of 11.00 to 11.51. The SHOBS buffer treated samples show a pH dependent functionality loss, presenting the highest functionality at 11.00 and the lowest with 11.51. The SHOBS buffer with a pH of 11.20, used in the previous experiments showed a reduction of 80% of functionality comparing to the EV sample that was only illuminated. Two different buffers, An HCl-Glycine 1M pH 3.00 and Formic acid 1% in PBS pH 3.00 were tested according to literature[48,63]. Both buffers were neutralized with a Tris 1M solution with a pH of 8. The Formic acid buffer barely presented a system activation. This may have occurred because the buffer was not properly neutralized. This was noticed by a change of color in the wells were it was added, although it also presented the lowest mCherry cell count from all conditions visualized by fluorescence microscopy. The HCl-Glycine buffer however, showed similar activation of the system as the SHOBS buffer with a pH of 11.23.

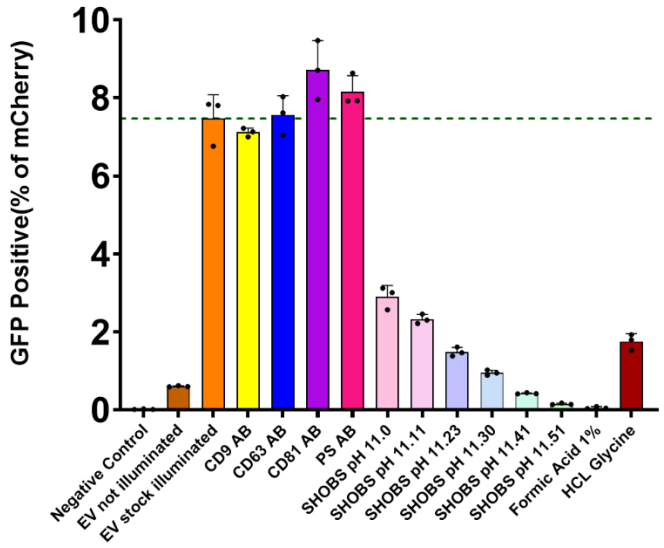


Figure 3.6. EV functionality loss was dependent on the pH of the elution buffer. HEK293T EVs were eluted with SHOBS buffer in a pH range of 11.00 to 11.51 and added to HEK293TSL reporter cells for flow cytometry analysis. Antibody controls (CD9 AB, CD63 AB, CD81 AB and PS AB), EVs only treated with the designated antibodies, were diluted with PBS to maintain the same particle concentration with the remaining samples. Elution buffer samples were treated for 5 minutes and then neutralized to a pH 7.4. All samples were UV-illuminated for 20 minutes except the EV sample not illuminated that was maintained on ice in the room.

## 3.6 The time of incubation of the SHOBS elution buffer does not affect the elution

In search to reduce the loss of functionality caused by the pH of the elution buffer we tried to reduce the incubation time. HEK293T EVs subpopulations were isolated according to the section 2.6 and treated with SHOBS buffer with different incubation times. The observed time of incubation had little to no effect on the elution of EVs out of the beads. A value of 90% of elution was observed after 0 minutes of incubation time. It differed however by 10% on the CD9+ and CD81+ subpopulations (Figure 3.7.). The maximum value of elution in all subpopulations was reached after 1 minute of incubation. With these results, we concluded that the incubation time did not affect the EV elution. For this reason, 1 minute of incubation time was tested in further experiments.

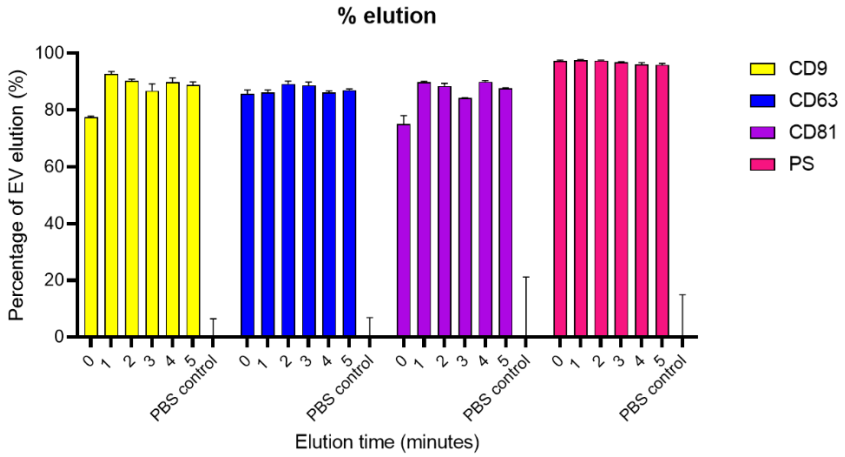


Figure 3.7. Incubation time with the elution buffer did not affect the elution of the subpopulations. After subpopulations isolation magnetic beads were incubated with the elution buffer with the different time ranges tested and afterwards dyed with PKH67 and analyzed by flow cytometry.

## 3.7 Reduced incubation time decreased the functionality loss

Prior we understood how the incubation time did not affect the elution of EV subpopulations out of the magnetic beads. The next step would be discerning how it could affect the functionality of the subpopulations. From previously obtained results in this project by Sander and previous student, we knew that our elution buffer caused damage to the functionality of the EVs depending on the incubation time. However, incubation times as low as the previous experiment were never tested before. HEK293T EVs were incubated with different incubation time, added to the HEK293TSL cells and analyzed by flow cytometry. The SHOBS buffer showed a functionality damage dependent on the incubation time (Figure 3.8.). The activation of the system decreased by extending the incubation time. An incubation time of 1 minute

with the SHOBS buffer showed a signal reduction of around 26% while an incubation time of 5 minutes resulted in a reduction of almost 80% of the reporter cells activation. Other buffers from literature were tested once again[48,63]. The formic acid 1% buffer showed almost a total loss of functionality similar to the negative control, even when the neutralization was done correctly. HCl-Glycine buffer however, showed a loss of 50% of functionality, leading to a better activation compared to an incubation time of 5 minutes with the SHOBS elution buffer. The Glycine buffer however still has a lower activation when comparing it to an incubation of 1 minute with the SHOBS elution buffer.

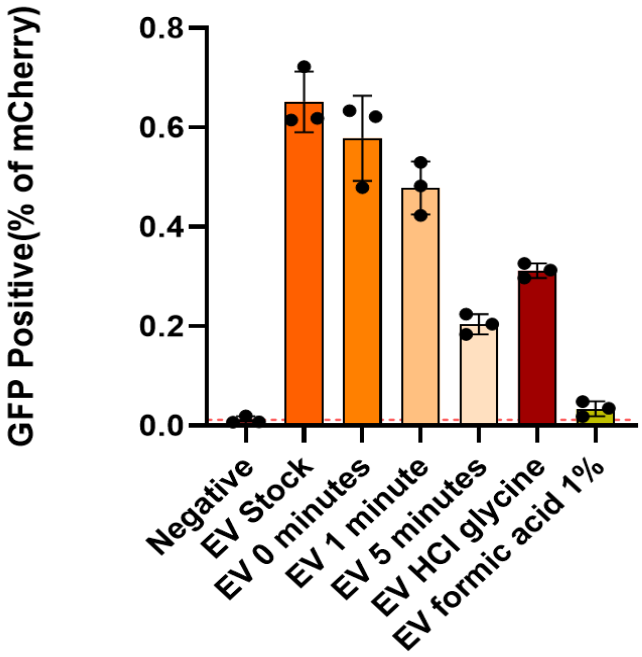


Figure 3.8. Incubation time of 1 minute reduced the functionality loss of the EVs compared to longer incubation times. HEK293T EVs with the same particle concentration were incubated with the respective elution buffer for the designated incubation time and neutralized to a pH of 7.4. EV samples were added to HEK293TSL cells and analyzed 3 days after the addition of the samples to the reporter cells by flow cytometry.

## 3.8 Enriching CD9 vesicles with RNA-Protein complex did not improve report cell activation

After optimization of the subpopulations elution, we tried to understand if any subpopulations exhibited an increased efficiency in RNA delivery. The used anchor for therapeutic content loading was a recombinant protein CD9-PhoCl-MS2, to achieve similar results, previously obtained in this project. EV isolation and subpopulation isolation was done as described in sections 2.2 and 2.6 while for normalization a MemGlow staining was done according to the methods. For the elution, 1 minute of incubation time was used for all EV samples in this

experiment with the SHOBS buffer. The obtained results (Figure 3.9.) did not show any activation of the system for most of the isolated subpopulations. Except for the CD81+ subpopulation, none of the other subpopulations showed activation above background. However, both supernatant of CD9+ and CD81+ subpopulations were depleted of active content. Since the CD63+ supernatant showed an activation of the system higher than the EV stock, it was considered a technical error. This may have been caused by adding the wrong sample to the wells or a contamination in between wells. PS+ subpopulation only showed activation of the system in the supernatant with a 50% loss of activation in comparison to the highest dose of the EV stock. The EV stock shows the maximum activation possible of the system with an activation of 0.5% and a dose dependent activation, as previously noted. Antibody controls were also done by treating the EV sample with the SHOBS buffer and antibodies but no magnetic beads and added in the same concentration as the highest dose of the EV stock. All antibody controls showed an activation reduction of 50% in comparison to the EV stock at the highest dose with the same concentration. This activation reduction of the system was higher than what was expected from what we had seen in previous results (Figure 3.8.).

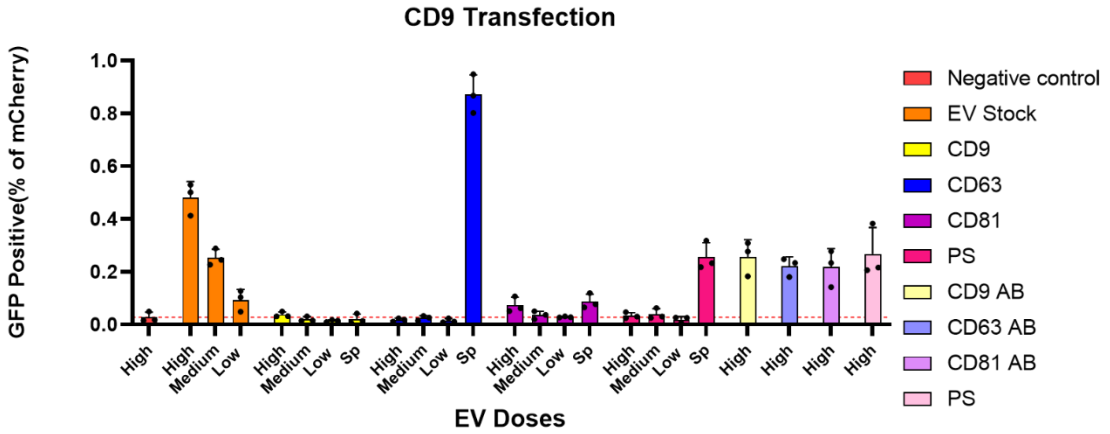


Figure 3.9. CD9 enriched EVs did not improve activation of the system. The functionality of EV subpopulations derived from HEK293T cells transfected with plasmids encoding for VSV-G, Cas9, sgRNA with MS2 aptamers and Myr-PhoCl-MS2 was compared in three doses (low= 1063.68 MFI , medium=2127.28, high=4254.55 Memglow590-derived fluorescence)by the expression of eGFP by HEK293T stoplight cells that was analyzed by flow cytometry 3 days after adding the samples to the cells. Supernatant samples (SP), obtained after isolation the specific subpopulation and antibody controls (AB) done by incubating the EV sample with the subpopulation antibody and the SHOBS elution buffer were added to the HEK293TSL reporter cells in the same concentration as the highest dose of the EV stock. Supernatant samples (Sp) were obtained after subpopulation isolation and dilluted to the same particle yield as the EV stock.

## 3.9 Analysis of EV subpopulation uptake

To find another readout for EV functionality of different subpopulations, a scratch assay was done with CPC EVs as they present innate ability to promote angiogenesis and cell migration.

Extracellular vesicles from cardiac progenitor cells (CPCs) were used in this experiments. CPCs have been reported to have the innate ability to promote cell migration on endothelial cells. This way, it is possible to evaluate the EV uptake by analyzing the migration done by endothelial cells, thus allowing to evaluate the delivery of different EV subpopulations. The maximum time of 6 hours was used since it was the maximum time point where the positive control cells did not fully migrate. CPC EVs and EV subpopulations were isolated according to the sections 2.2 and 2.6, respectively, and added to HMEC-1-eGFP cells after scratching the cells. HMEC-1 eGFP cells were used as a reporter system, with a confluency of 40.000 cells per well. Photos were taken after adding the samples to the cells. The first time point t1 = 0 was considered to be the moment of the first picture taken and t2 = 6 hours after the t1 (Figure 3.10.).

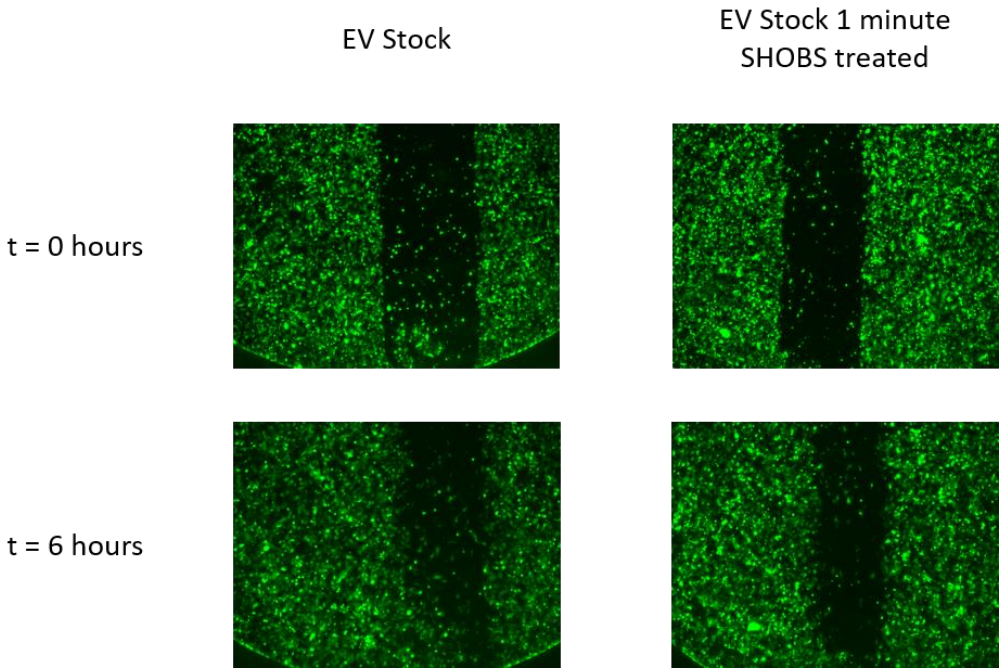


Figure 3.10. Pictures taken at t = 0 hours and t = 6 hours of the cells treated with the EV stock on the left and the EV sample treated 1 minute with the SHOBS elution buffer on the right.

In this experiment, we tried to normalize our samples by fluorescence normalization. However, the process of purifying our sample off the unbound dye, greatly reduced our EV yield which disabled us from using these samples for any further experiments since a particle concentration below 1E+08 particles was previously seen to not cause any regrowth of the wound. Therefore, subpopulation samples were discarded due to their low particle concentration. Nonetheless, supernatant and antibody controls, were still obtained and analyzed. From the obtained results (Figure 3.11.a) we can see that most of the samples did not present a cell migration above the negative control, sample not incubated with any EV sample and neither

incubated with medium supplemented with growth factors. The regrowth percentage observed in Figure 3.11.a. showed the absolute regrowth when comparing the cells at t1 and t2. The total difference of area of pixel was obtained by subtracting the area of pixel at t1 by t2 (Figure 3.11.b.). Both analysis of cell migration show that most samples were not able to have a cell migration superior to the cell migration that occurred in the negative control. Although the EV stock showed some variability, it showed higher cell migration comparing to the negative control.

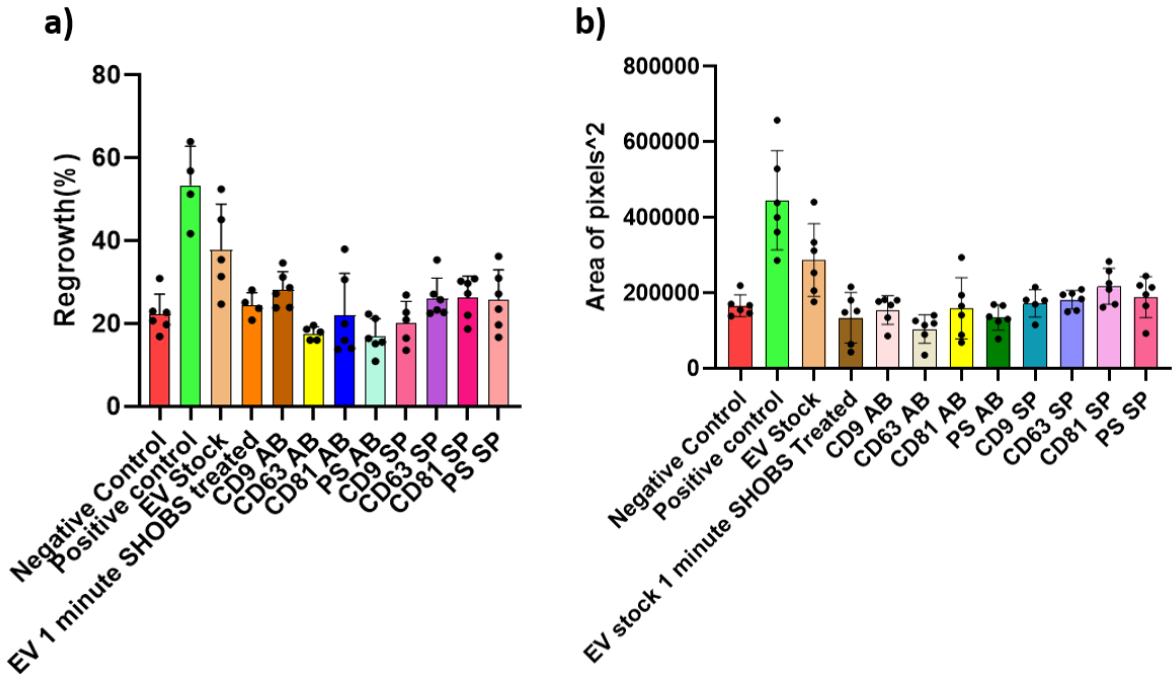


Figure 3.11. Analysis of the cell migration of HMEC-1 eGFP cells after addition of CPC EVs. CPC-derived EVs were isolated and treated with SHOBS buffer for 1 minute. Antibody controls (AB), for analysis of the effect of the antibody presence, were done by incubating CPC EVs with the specified antibody targeting subpopulation markers, and treated with SHOBS buffer for 1 minute. EVs were added to the cells (2.12E+09 particles per well) on a 96 well plate and analyzed at t1 = 0 hours and t2 = 6 hours. a) Regrowth percentage calculated according the established formula. b) Comparison of the area of pixel by the subtraction of t1 = 0 hours by t2 = 6 hours.

# 4 Discussion

The goal of this study was to understand how functional EV-mediated RNA transfer and interaction with the cells of different EV subpopulations occurs for future development of a drug delivery system. Previously, Sander Kooijmans and previous students created a stable elution buffer with the pH of 11.20. The pH of 11.20 was chosen out of the tested pH range since it showed the best elution/damage ratio. Lower pH showed a poor elution while a higher pH increased EV functionality loss. These results were verified (Figure 7.) in search of further optimizing the protocol. Results from previous students of this project were not presented here even though they were used as basic knowledge for the obtained results. Y. Cheng et al 2019 showed that the temperature and pH at which the EVs are stored, influences the representative levels of theirs markers[64]. The highest levels were found when stored at 4$^{o}$C in a neutral pH. In this project, all used EVs were considered fresh, since they were used within a maximum of four days after isolation. EVs were stored in neutral solution to maintain them stable and as active as possible for functionality tests. The elution buffer used has a far more basic pH than the one from the article[64]. Hence, it could show an increased loss of functionality in our results, however, neutralization was done after maximum 5 minutes of incubation, to reduce the loss of EV functionality. Other point to notice on this project, is the used technique to quantify the particle concentration for subpopulation pulldown. For this step, NTA was used. This method can present some issues. Since it counts all particles present in the solution and not only the desired extracellular vesicles, it causes an overestimation of the EVs since we assume that all the particles counted were EVs. Tests should have been done to understand if the Memglow590 dye used would be equally distributed over all EV subpopulations. Doing a Fluorescence based normalization when the dye was not equally distributed over the EV subpopulations, could cause the addition of different concentrations of EV subpopulations to the cells by differences in the dye distribution where the fluorescence would be the same in all EV subpopulations.

## 4.1 Enriched CD81 vesicles show higher system activation of the CD9+ EV subpopulation

The CROSS-FIRE system was chosen for this project for its ability to detect RNA delivery with high sensivity[25]. Analysis by flow cytometry enables us to count the cells that co-express mCherry and eGFP. The eGFP expression originated from the Cas9/sgRNA delivery to the

nucleus of the cell at any timepoint in the past, hence we are able to analyze the efficiency of the EV-mediated RNA delivery. The sgRNA-Cas9 complex was loaded into EVs using a CD81 recombinant protein anchor. After transfection, the cells will overexpress the recombinant protein anchor with the desired tetraspanin in cell membranes and further form extracellular vesicles with the anchor in the surface. Since the anchor presents a MS2 aptamer binding protein, it is able to bind the MS2 aptamers of the sgRNA, which allows for an efficient loading of the EVs. The results were analyzed by comparing the different subpopulations to the EV stock. Considering the normalization based on particles, our EV stock was full of non-EV particles when compared to the EV subpopulations, which were pure EV samples. When the normalization by Memglow590-derived fluorescence is done all lipids are dyed, which should improve the normalization compared to the use of NTA for normalization, nonetheless, some non-EV contaminants could still be present. This would cause an overestimation of the amount of EVs that are being added to the cells, as the amount is lower than what we had forseen, thus causing a reduced reporter cell activation than what we would expect. The results had shown that the highest system activation occurred when CD9+ EVs were added with the high and medium dose, followed by the CD81+ EVs (Figure 2.) From these results, we could consider that CD9+ and CD81+ subpopulations would have an increased RNA delivery efficacy. However, the CD81 anchor would overexpress the CD81 tetraspanin, thus, influencing the obtained results. The CD9 tetraspanin presents the same origin in the cell coming from the same budding membrane[44], which may have caused an overexpression of CD81+ on the CD9+ subpopulation. Hence, the CD9 subpopulation would present a higher load of the active content. This would lead to a higher activation of the system by the higher active content in the subpopulation. We considered that the overexpression of CD81 might have caused an inefficient elution from the magnetic beads for the CD81 subpopulation. The overexpression of the CD81 tetraspanin will cause the EVs to bind strongly to the magnetic beads due to the increase of antibodies attached to a single vesicle.

## 4.2 Myr engineered EVs were not isolated in the EV subpopulations

To improve the equal loading of the active content in the EV subpopulations or reduce the effect of the anchor on the active content distribution we used a myristoylation anchor. The results showed an efficient isolation of the EV subpopulations, observed in the Western blot, since the HA-Tag, expressed in the encoded recombinant protein, was present in the subpopulation in lower concentration compared to the supernatant samples. This suggested that we were not able to isolate the Myr engineered EVs in the EV subpopulations. This was confirmed

by the lack of system activation on the subpopulation doses and to a maximum activation of the system on the supernatant samples. The active content was not isolated or our elution buffer destroyed it. Although we knew that a basic elution buffer would damage the EVs to some extent, it was not expected to destroy the total activity of the EVs. Repetitions of the experiment kept showing activity almost exclusively in the supernatant samples. Previous results had already showed functional activity from the subpopulations with different used anchors, hence the system should not be affected by the different anchor used. We tried to understand how to optimize our methods to improve the system activation. As such, we aimed to understand how the VSV-G affected the EV elution. From Whitley et al.2022 we knew that VSV-G would increase the size of vesicles when transfected to the cells[9]. We also suspected that expressed VSV-G could affect the natural EV properties and decrease the elution efficacy[65].

## 4.3 Effect of VSV-G on elution

We next aimed to understand how the VSV-G could affect the subpopulation isolation. Extracellular vesicles with and without VSV-G and subpopulations were isolated and the respective magnetic beads analyzed (Figure 5.). The VSV-G EV beads showed a lower capture compared to the EVs without VSV-G. The obtained results showed that the VSV-G was affecting the total capture of EVs by the magnetic beads. The expression of VSV-G was known to promote an exceeded release of EVs[66]. Some of the released EVs would present VSV-G, while other EVs would be considered more virus-like particles with a great VSV-G expression but no EV characteristics. The virus-like particles would also be counted in the NTA normalization as if they were EVs. This would cause the increased addition of EVs to the beads in samples without VSV-G expression compared to EVs expressing VSV-G, thus causing a lower capture efficiency. Although VSV-G increases the RNA delivery efficacy of the EVs as seen by Somiya et al.2021, we tried to remove this viral protein in order to increase the efficiency of the subpopulation isolation[10].

## 4.4 The VSV-G expression was necessary for the CROSS-FIRE System activation

From literature we knew that HEK293T EVs presented a functional delivery of content dependent of VSV-G, as such to test the activation of the system without VSV-G we choose HeLa EVs[10]. HeLa cells are easy to culture and maintain. Subpopulation isolation with HeLa EVs was not done before validating that HeLa EVs were able to activate the system without VSV-

G. The results showed that it was not possible to activate the system above background. Although when expressing VSV-G in the EVs, we saw activation of the system similar to the activation seen in the positive control, where cells were directly transfected with sgRNA and Cas9. We concluded that HeLa EVs were not able to escape endosomal degradation without VSV-G. Even if they did, they were not able to reach the nuclei and cause the frameshift for eGFP expression. It was considered that VSV-G could be hiding the delivery effect of the different subpopulation. The differences in EV subpopulation delivery efficacy would only be due to the overexpression of VSV-G in some subpopulations. However, western blot results (Figure 4.) did not support this theory, since the VSV-G band was equally present in the EV samples and the activation still differed as seen previously. For this reason, VSV-G was maintained in further experiments to have a considerable activation of the system. It is important to note that HeLa cells were only used in this experiment and the following results were obtained with HEK293T EVs since they were easier to transfect than HeLa cells.

## 4.5 EV-mediated RNA delivery showed functional loss dependent of the elution buffer pH

Since it was impossible to remove VSV-G expression if we wanted to have significant reporter cell activation, we searched for a different way to improve the activation of the system. To check what else could be affecting the reporter cells activation by EV-mediated RNA delivery, we incubated EV samples with antibodies or with the SHOBS elution buffer in a pH range of 11.00-11.51. The activation of the system was not affected when the EVs were incubated only with the antibodies used for the subpopulation isolation, since the reporter cells had shown an activation on the same level as the EV stock. However when the EVs were not illuminated, the active construct still remained bound to the anchor used for loading. This caused a 90% reduction of the activation of the reporter cells compared to when the EV sample was illuminated, which illustrated the importance of UV-illumination for the release of the cargo from the EV surface for it to be functional. When the EV samples were incubated with the SHOBS elution buffer, the samples showed a decreasing activation of the system with the increasing pH of the elution buffer. We theorized that the incubation with the elution buffer caused the EV surface to open. The high pH of the elution buffer would cause some loss of functionality of the active content inside the EV. We know that RNA may suffer alkaline hydrolysis when the pH is superior to 6, as such the use of a high pH such as 11.20 may cause the degradation of the sgRNA[67]. For the Cas9 protein, no pH effect was described in the literature. However, the reduction of reporter cells activation, observed in the antibody controls samples incubated

with the SHOBS buffer was observed to be minimal, which may indicate that the loss of functional delivery occurs due to the magnetic beads, since they were not used in antibody controls. No studies were done to further comprehend the effect of the magnetic beads on the EV yield, other beads should be tested to understand how their use can influence the EV subpopulations yield. Two elution buffers from literature were also tested to compare how the buffer and the pH could affect the functionality of the EV-mediated RNA delivery by the reporter cells activation compared to our SHOBS buffer. The Formic acid 1% elution buffer treated EVs presented a minimal activation of the reporter cells. The lack of activation could have been due to the death of the cells because of the low pH of the buffer as it was shown by the photos taken of the cells (Figure 6.1.). HCl-Glycine treated EVs showed a similar activation as the SHOBS buffer for a pH of 11.21 and could be considered a better buffer compared to the one designed in this project. Nonetheless, the SHOBS buffer was created previously on this project and not fully optimized. So it was decided to further explore the possibility to optimize our elution buffer.

## 4.6 The incubation time does not affect the EV elution

To further optimize the protocol use of the SHOBS elution buffer, we searched to understand how the incubation time could affect the elution of the EVs from the magnetic beads. We previously knew that the elution buffer would cause functionality damage depending on the incubation time from previous research on this project. However, no research was done until now on how it could affect the elution from the magnetic beads at such reduced incubation times. The EV samples were incubated with the designed antibodies for isolation of each subpopulation for 24 hours. Afterwards, the beads were washed and eluted with the SHOBS elution buffer for the designated incubation time. Results showed that the elution from the magnetic beads was almost instantaneous. Although, lower elution percentages were seen In the CD9+ and CD81+ EV subpopulation in the 0 minute incubation sample compared to CD63+ and PS+ EV subpopulation with 0 minutes of incubation. The CD63+ and PS+ EV subpopulations may have been incubated for a longer time than others in the 0 minutes samples, which may have occurred due to discrepancies in the speed of transferring the neutralization buffer to the sample. Nevertheless, all subpopulations seem to have reached a 90% elution after 1 minute of incubation.

## 4.7 EV functional loss was dependent on the incubation time

The use of SHOBS buffer showed no effect on the elution of the vesicles after 1 minute of incubation time. However, previous experiments on this project indicated that the functionality damage was dependent on the incubation time. Experiments with such reduced incubation time had not been done until now, since the elution buffer was only tested with times ranging from 5 minutes to 30 minutes. When the EV sample was incubated for 1 minute with the SHOBS buffer, it showed an activation reduction of 26% compared to the EV stock that was used as control and not incubated with any elution buffer. An increase in activity loss of 80% was seen for the sample incubated for 5 min with the SHOBS buffer in comparison to the activity of the control sample. These results indicate that the functionality damage was greatly dependent on the incubation time with the elution buffer. Samples were not incubated with any antibodies for the subpopulation isolation, although, antibody incubation could increase the functionality damage, this was not proven with the obtained results. Reducing the incubation time to 1 minute would allow a reduction of the functionality damage to a minimum while maintaining the maximum yield possible. This functionality damage was due to the basic pH that caused a reduction in the obtained total yield[64]. The formic acid 1% elution buffer was tested to compare to the SHOBS buffer[63]. As previously seen, the activation was around background levels. On the previous experiment with this buffer, most of the cells died as seen on the taken microscopic images. To have an equal neutralization with all buffers, a titration curve was done in order to obtain the correct neutralization. Nonetheless, results remained the same and the activation of the system persisted on the same levels. This could indicate that the pH of the buffer would cause a higher loss of functionality. Once more, the HCl-Glycine showed a higher activation of the system than incubation with SHOBS elution buffer for 5 minutes[48]. There was a total difference of 30% between the two samples. These results had previously caused doubt on the use of the SHOBS buffer. However, after optimization it showed a higher efficiency with 1 minute of incubation since the activation was 24% higher than the sample incubated with HCl-Glycine. As such, it was concluded that the HCl-Glycine elution buffer would not be the preferred one for the functionality tests. From the obtained results, we decided to shorten the incubation time with the elution buffer to 1 minute in the posterior experiments.

## 4.8 Enriching CD9 vesicles with RNA-Protein complex did not improve reporter cell activation

Functionality experiments were repeated again after the optimization of the elution buffer throughout the project. The CD9-PhoCl-MS2 plasmid was used instead of a myristoylation plasmid since previously, we were not able to isolate the Myr enriched EVs on the isolated EV subpopulations. The CD9+ and CD81+ subpopulations are formed in the same budding membrane causing an overlap of these tetraspanins in their EV subpopulations[44]. In the obtained results, all EV subpopulations added to the reporter cells presented an activation of the system similar to background reporter cells activation, which was lower than what we expected. The CD9+ and CD81+ EV subpopulations added to the reporter cells presented an activation of the system similar to the negative control, in which the cells were only treated with SHOBS buffer and the Tris-HCl neutralization buffer in a SHOBS/Neutralization buffer ratio of 1:0.15. However, the supernatant samples from the CD9+ and CD81+ subpopulations showed an almost total depletion of signal. This suggested that some problem with the neutralization of the buffer must have occurred or some technical error that caused the lack of reporter cell activation from CD9+ and CD81+ EVs. CD9 enriched vesicles showed the highest activation for the CD81+ EV subpopulation, while comparing to the CD81 enriched vesicles results, showed the CD9+ subpopulation to be the highest. As previously seen, it is not the subtype of the transfected anchor that presents the highest activation, but the one formed in the same membrane. Nevertheless, due to the overexpression of the transfected anchor, the subpopulation will develop an overexpression of the CD9 tetraspanin on the membrane of the vesicle. This would cause a high affinity binding of the incubated antibodies resulting in a multiple antibodies binding to a single vesicle and an inefficient elution. This resulted in a reduced yield of EVs of the subpopulation presenting the same tetraspanin, and a reduction in the loaded vesicle, causing a decrease in the activation observed. Sander repeated this experiment and showed a much higher activation signal than the one we were able to obtain in this experiment. This confirmed that something must have occurred on the performed experiment (results not shown). Technical errors, problems with the elution or neutralization of the buffer could have happened, which caused a higher loss of functionality damage than expected. Although we know some mistakes must have happened, the discussion will only cover the obtained results. Antibody controls also showed a 50% reduction of activation when compared to the highest dose of our EV stock control. The decrease in the activation was higher than what we had previously seen, which further proved that some technical error must have happened in the experiment. Since we were not able to obtain any conclusion from this experiment we aimed

for a different experiment to compare the functional RNA delivery efficiency of different EV subpopulations.

## 4.9 Wound healing assay

As a different way to analyze the RNA delivery efficacy of the EV subpopulation CPC EVs were used. According to Vrijsen et al. 2010, it was previously seen that CPC EVs had the ability to activate endothelial signaling pathways which stimulates the migration of HMEC-1 cells. Matrix metalloproteinase and extracellular matrix metalloproteinase inducer were found in CPC EVs [60]. This metalloproteinase presents an established role in the enchantment of angiogenesis and endothelial migration[61]. In this experiment, the EV yield obtained from CPCs was unfortunately much lower compared to HEK293T that are transfected with VSV-G. This resulted in the reduction of the sample particle concentration when normalizing it by fluorescence. Because of fluorescence-based normalization, another size exclusion chromatography was necessary to purify the EVs of the used unbound dye. This caused a big loss of yield that did not allow their use since the fluorescence signal obtained from each sample would greatly vary per acquisition. As such, only antibody controls and supernatant samples were considered to have a particle yield that was high enough to activate the migration of the cells. However, most of the samples showed identical levels of regrowth as the negative control sample where no EVs nor any growth factors were added to the cells. This suggests that the particle concentration was not high enough to induce a considerable migration of the cells.

# 5 Conclusion

In this project, we were not able to obtain an efficient RNA delivery for any of the isolated EV subpopulations, since the reporter cells activation was continuously low. However, they were still able to deliver the active content depending on the used anchor. Regardless, CD9+ and CD81+ subpopulations showed a higher reporter cell activation compared to the rest. The higher activation of these two subpopulations could be due to the use of CD9 and CD81 tetraspanin anchors that could be influencing the results because of their overexpression. The overexpression of the tetraspanin associated with the expressed anchor, could increase the affinity to the magnetic beads and reduce the efficiency of our isolation. However, the reporter cell activation was too high to be justified by the tetraspanin overexpression only. This suggests that CD9+ and CD81+ subpopulations may have a higher functional EV-mediated RNA delivery than other isolated subpopulations.

As a solution to reduce the influence of the used anchor, switchable nanobodies could be used as the ones presented in the Farrants et al. 2020[68]. In this article, they created a nanobody with affinity for green fluorescence proteins (GFP) and the binding affinity could be switched on and off with NADPH, causing a structural change of the bacterial enzyme, associated to the antibody[68]. This method could have been used to create a nanobody that would bind to the magnetic beads and present affinity to the used tetraspanin EV markers, without the use of an elution buffer with basic pH that can affect the reporter cells activation. However, for the use of this system, further tests would be necessary to understand how the small molecules used to control the binding affinity would affect our EV-mediated RNA delivery. Another option would be creating nanobodies that are similar to the one used for the isolation of the PS+ subpopulation in which the vesicles are captured using a R2-C1C2, an engineered antibody, incorporated with a Myc-tag[54]. This tag allows the use of anti-Myc antibodies which can bind to the magnetic beads. The use of this type of engineered nanobodies would allow an efficient release out of the magnetic beads, with the use of the elution buffer and exclude the possibility of interference of the antibodies on EV internalization as previously seen by Santos et al. 2019[65]. However, no impairment of the reporter cell activation was observed in the obtained results.
The used recombinant protein anchor should be equally distributed over all subpopulations, to reduce the influence of the overexpression of the anchor on the functional delivery of a specific EV subpopulation. The myristoylation anchor was used to achieve an equal distribution however, such results were not seen. The results suggested that myr enriched EVs were

not present in the isolated subpopulations, but in subpopulations not enriched with the targeted tetraspanins.

Other anchors could be used for equal distribution of the EV subpopulation, such as the palmitoylation anchor or other protein anchors that could be expressed on the surface of the vesicles but not common EV markers. Nevertheless, the anchor expressed should not affect the normal activity of the vesicles. If we could overcome the presented issues of subpopulation isolation and elution, we would improve the reporter cell activation and sensitivity of the CROSS-FIRE system.

Overall, we were able to analyze the RNA delivery efficacy of each tested EV subpopulation, even though the activation was lower than what was desired. We believe that if the experiments were to be repeated, higher activations of the system can be obtained. Nonetheless, different techniques could be used for analysis of RNA delivery, such as the repetition of the wound healing assay. The wound healing assay would allow to compare the EV uptake of the different subpopulations which could correlate to an efficient RNA delivery. However, CPC EVs promote cell migration by activation of different pathways associated with metalloproteinases and not associated with their delivery to the muclei. This may differ from the obtained results when using the CROSS-FIRE system, which shows reporter cell activation only when the sgRNA and Cas9 reach the nuclei and cause the frameshift for eGFP expression. Another technique possible for analysis of EV cargo delivery would be the Nanobit assay used in Somiya et al.2021[69]. In this EV cargo delivery assay, a split luciferase would be loaded in the EVs and reporter cells containing LgBiT, a large subunit of the luciferase, would emit luminescence when EV cargo proteins fused with a small luminescence tag and complement the LgBiT contained in the reporter cells. We believe, that the use of the methods explained would allow to confirm the data obtained in this project and show that no influence of the method use.

# REFERENCES


1. Pitt JM, Kroemer G, Zitvogel L. Extracellular vesicles: masters of intercellular communication and potential clinical interventions. Journal of Clinical Investigation. 2016;126(4):1139-1143. doi:10.1172/JCI87316
2. Yang Q, Xu J, Gu J, et al. Extracellular Vesicles in Cancer Drug Resistance: Roles, Mechanisms, and Implications. Advanced Science. 2022;9(34). doi:10.1002/advs.202201609
3. Havel H, Finch G, Strode P, et al. Nanomedicines: From Bench to Bedside and Beyond. AAPS J. 2016;18(6):1373-1378. doi:10.1208/s12248-016-9961-7
4. Savić N, Schwank G. Advances in therapeutic CRISPR/Cas9 genome editing. Translational Research. 2016;168:15-21. doi:10.1016/j.trsl.2015.09.008
5. de Voogt WS, Tanenbaum ME, Vader P. Illuminating RNA trafficking and functional delivery by extracellular vesicles. Adv Drug Deliv Rev. 2021;174:250-264. doi:10.1016/j.addr.2021.04.017
6. Sun H, Burrola S, Wu J, Ding WQ. Extracellular Vesicles in the Development of Cancer Therapeutics. Int J Mol Sci. 2020;21(17):6097. doi:10.3390/ijms21176097
7. O'Brien K, Breyne K, Ughetto S, Laurent LC, Breakefield XO. RNA delivery by extracellular vesicles in mammalian cells and its applications. Nat Rev Mol Cell Biol. 2020;21(10):585-606. doi:10.1038/s41580-020-0251-y
8. Kulkarni JA, Witzigmann D, Thomson SB, et al. The current landscape of nucleic acid therapeutics. Nat Nanotechnol. 2021;16(6):630-643. doi:10.1038/s41565-021-00898-0
9. Whitley JA, Kim S, Lou L, et al. Encapsulating Cas9 into extracellular vesicles by protein myristoylation. J Extracell Vesicles. 2022;11(4). doi:10.1002/jev2.12196

10. Somiya M, Kuroda S. Reporter gene assay for membrane fusion of extracellular vesicles. J Extracell Vesicles. 2021;10(13). doi:10.1002/jev2.12171
11. Jurgielewicz BJ, Yao Y, Stice SL. Kinetics and Specificity of HEK293T Extracellular Vesicle Uptake using Imaging Flow Cytometry. Nanoscale Res Lett. 2020;15(1):170. doi:10.1186/s11671-020-03399-6
12. Kooijmans SAA, de Jong OG, Schiffelers RM. Exploring interactions between extracellular vesicles and cells for innovative drug delivery system design. Adv Drug Deliv Rev. 2021;173:252-278. doi:10.1016/j.addr.2021.03.017
13. Sridharan K, Gogtay NJ. Therapeutic nucleic acids: current clinical status. Br J Clin Pharmacol. 2016;82(3):659-672. doi:10.1111/bcp.12987
14. Tenchov R, Bird R, Curtze AE, Zhou Q. Lipid Nanoparticles─From Liposomes to mRNA Vaccine Delivery, a Landscape of Research Diversity and Advancement. ACS Nano. 2021;15(11):16982-17015. doi:10.1021/acsnano.1c04996
15. Gostimskaya I. CRISPR–Cas9: A History of Its Discovery and Ethical Considerations of Its Use in Genome Editing. Biochemistry (Moscow). 2022;87(8):777-788. doi:10.1134/S0006297922080090
16. Kuhn J, Lin Y, Krhac Levacic A, et al. Delivery of Cas9/sgRNA Ribonucleoprotein Complexes via Hydroxystearyl Oligoamino Amides. Bioconjug Chem. 2020;31(3):729-742. doi:10.1021/acs.bioconjchem.9b00853
17. Horvath P, Barrangou R. CRISPR/Cas, the Immune System of Bacteria and Archaea. Science (1979). 2010;327(5962):167-170. doi:10.1126/science.1179555
18. Evers MJW, Kulkarni JA, van der Meel R, Cullis PR, Vader P, Schiffelers RM. State-of-the-Art Design and Rapid-Mixing Production Techniques of Lipid Nanoparticles for Nucleic Acid Delivery. Small Methods. 2018;2(9). doi:10.1002/smtd.201700375
19. Evers MJW, van de Wakker SI, de Groot EM, et al. Functional siRNA Delivery by Extracellular Vesicle–Liposome Hybrid Nanoparticles. Adv Healthc Mater. 2022;11(5). doi:10.1002/adhm.202101202
20. Wu P, Zhang B, Ocansey DKW, Xu W, Qian H. Extracellular vesicles: A bright star of nanomedicine. Biomaterials. 2021;269:120467. doi:10.1016/j.biomaterials.2020.120467
21. Wang BZ, Luo LJ, Vunjak-Novakovic G. RNA and Protein Delivery by Cell-Secreted and Bioengineered Extracellular Vesicles. Adv Healthc Mater. 2022;11(5). doi:10.1002/adhm.202101557
22. Roefs MT, Sluijter JPG, Vader P. Extracellular Vesicle-Associated Proteins in Tissue Repair. Trends Cell Biol. 2020;30(12):990-1013. doi:10.1016/j.tcb.2020.09.009
23. Narauskaitė D, Vydmantaitė G, Rusteikaitė J, et al. Extracellular Vesicles in Skin Wound Healing. Pharmaceuticals. 2021;14(8):811. doi:10.3390/ph14080811

24. Mateescu B, Kowal EJK, van Balkom BWM, et al. Obstacles and opportunities in the functional analysis of extracellular vesicle RNA – an ISEV position paper. J Extracell Vesicles. 2017;6(1). doi:10.1080/20013078.2017.1286095
25. de Jong OG, Murphy DE, Mäger I, et al. A CRISPR-Cas9-based reporter system for single-cell detection of extracellular vesicle-mediated functional transfer of RNA. Nat Commun. 2020;11(1):1113. doi:10.1038/s41467-020-14977-8
26. Nicolás-Ávila JA, Lechuga-Vieco A V., Esteban-Martínez L, et al. A Network of Macrophages Supports Mitochondrial Homeostasis in the Heart. Cell. 2020;183(1):94-109.e23. doi:10.1016/j.cell.2020.08.031
27. Teng F, Fussenegger M. Shedding Light on Extracellular Vesicle Biogenesis and Bioengineering. Advanced Science. 2021;8(1). doi:10.1002/advs.202003505
28. Ratajczak J, Miekus K, Kucia M, et al. Embryonic stem cell-derived microvesicles reprogram hematopoietic progenitors: evidence for horizontal transfer of mRNA and protein delivery. Leukemia. 2006;20(5):847-856. doi:10.1038/sj.leu.2404132
29. Lee JM, Yoon TJ, Cho YS. Recent Developments in Nanoparticle-Based siRNA Delivery for Cancer Therapy. Biomed Res Int. 2013;2013:1-10. doi:10.1155/2013/782041
30. Biagiotti S, Abbas F, Montanari M, et al. Extracellular Vesicles as New Players in Drug Delivery: A Focus on Red Blood Cells-Derived EVs. Pharmaceutics. 2023;15(2):365. doi:10.3390/pharmaceutics15020365
31. Catalano M, O'Driscoll L. Inhibiting extracellular vesicles formation and release: a review of EV inhibitors. J Extracell Vesicles. 2020;9(1). doi:10.1080/20013078.2019.1703244
32. Willms E, Cabañas C, Mäger I, Wood MJA, Vader P. Extracellular Vesicle Heterogeneity: Subpopulations, Isolation Techniques, and Diverse Functions in Cancer Progression. Front Immunol. 2018;9. doi:10.3389/fimmu.2018.00738
33. Mallia A, Gianazza E, Zoanni B, Brioschi M, Barbieri SS, Banfi C. Proteomics of Extracellular Vesicles: Update on Their Composition, Biological Roles and Potential Use as Diagnostic Tools in Atherosclerotic Cardiovascular Diseases. Diagnostics. 2020;10(10):843. doi:10.3390/diagnostics10100843
34. Crescitelli R, Lässer C, Jang SC, et al. Subpopulations of extracellular vesicles from human metastatic melanoma tissue identified by quantitative proteomics after optimized isolation. J Extracell Vesicles. 2020;9(1). doi:10.1080/20013078.2020.1722433
35. Kowal J, Arras G, Colombo M, et al. Proteomic comparison defines novel markers to characterize heterogeneous populations of extracellular vesicle subtypes. Proceedings of the National Academy of Sciences. 2016;113(8). doi:10.1073/pnas.1521230113

36. Acevedo-Sánchez V, Martínez-Ruiz R, Aguilar-Ruíz S, et al. Quantitative Proteomics for the Identification of Differentially Expressed Proteins in the Extracellular Vesicles of Cervical Cancer Cells. Viruses. 2023;15(3):702. doi:10.3390/v15030702
37. Cvjetkovic A, Jang SC, Konečná B, et al. Detailed Analysis of Protein Topology of Extracellular Vesicles–Evidence of Unconventional Membrane Protein Orientation. Sci Rep. 2016;6(1):36338. doi:10.1038/srep36338
38. Théry C, Witwer KW, Aikawa E, et al. Minimal information for studies of extracellular vesicles 2018 (MISEV2018): a position statement of the International Society for Extracellular Vesicles and update of the MISEV2014 guidelines. J Extracell Vesicles. 2018;7(1). doi:10.1080/20013078.2018.1535750
39. Friand V, David G, Zimmermann P. Syntenin and syndecan in the biogenesis of exosomes. Biol Cell. 2015;107(10):331-341. doi:10.1111/boc.201500010
40. Bobrie A, Colombo M, Krumeich S, Raposo G, Théry C. Diverse subpopulations of vesicles secreted by different intracellular mechanisms are present in exosome preparations obtained by differential ultracentrifugation. J Extracell Vesicles. 2012;1(1). doi:10.3402/jev.v1i0.18397
41. Jankovičová J, Sečová P, Michalková K, Antalíková J. Tetraspanins, More than Markers of Extracellular Vesicles in Reproduction. Int J Mol Sci. 2020;21(20):7568. doi:10.3390/ijms21207568
42. Tognoli ML, Dancourt J, Bonsergent E, et al. Lack of involvement of CD63 and CD9 tetraspanins in the extracellular vesicle content delivery process. Commun Biol. 2023;6(1):532. doi:10.1038/s42003-023-04911-1
43. Fan Y, Pionneau C, Cocozza F, et al. Differential proteomics argues against a general role for CD9, CD81 or CD63 in the sorting of proteins into extracellular vesicles. J Extracell Vesicles. 2023;12(8). doi:10.1002/jev2.12352
44. Mathieu M, Névo N, Jouve M, et al. Specificities of exosome versus small ectosome secretion revealed by live intracellular tracking of CD63 and CD9. Nat Commun. 2021;12(1):4389. doi:10.1038/s41467-021-24384-2
45. Silva AM, Lázaro-Ibáñez E, Gunnarsson A, et al. Quantification of protein cargo loading into engineered extracellular vesicles at single-vesicle and single-molecule resolution. J Extracell Vesicles. 2021;10(10). doi:10.1002/jev2.12130
46. Liangsupree T, Multia E, Riekkola ML. Modern isolation and separation techniques for extracellular vesicles. J Chromatogr A. 2021;1636:461773. doi:10.1016/j.chroma.2020.461773
47. Oksvold MP, Neurauter A, Pedersen KW. Magnetic Bead-Based Isolation of Exosomes. In: ; 2015:465-481. doi:10.1007/978-1-4939-1538-5_27

48. Karimi N, Dalirfardouei R, Dias T, Lötvall J, Lässer C. Tetraspanins distinguish separate extracellular vesicle subpopulations in human serum and plasma – Contributions of platelet extracellular vesicles in plasma samples. J Extracell Vesicles. 2022;11(5). doi:10.1002/jev2.12213
49. Sidhom K, Obi PO, Saleem A. A Review of Exosomal Isolation Methods: Is Size Exclusion Chromatography the Best Option? Int J Mol Sci. 2020;21(18):6466. doi:10.3390/ijms21186466
50. Record M, Carayon K, Poirot M, Silvente-Poirot S. Exosomes as new vesicular lipid transporters involved in cell–cell communication and various pathophysiologies. Biochimica et Biophysica Acta (BBA) - Molecular and Cell Biology of Lipids. 2014;1841(1):108-120. doi:10.1016/j.bbalip.2013.10.004
51. Han Y, Jones TW, Dutta S, et al. Overview and Update on Methods for Cargo Loading into Extracellular Vesicles. Processes. 2021;9(2):356. doi:10.3390/pr9020356
52. Breyne K, Ughetto S, Rufino-Ramos D, et al. Exogenous loading of extracellular vesicles, virus-like particles, and lentiviral vectors with supercharged proteins. Commun Biol. 2022;5(1):485. doi:10.1038/s42003-022-03440-7
53. Shadish JA, Strange AC, DeForest CA. Genetically Encoded Photocleavable Linkers for Patterned Protein Release from Biomaterials. J Am Chem Soc. 2019;141(39):15619-15625. doi:10.1021/jacs.9b07239
54. Kooijmans SAA, Gitz-Francois JJJM, Schiffelers RM, Vader P. Recombinant phosphatidylserine-binding nanobodies for targeting of extracellular vesicles to tumor cells: a plug-and-play approach. Nanoscale. 2018;10(5):2413-2426. doi:10.1039/C7NR06966A
55. Llorente A, Skotland T, Sylvänne T, et al. Molecular lipidomics of exosomes released by PC-3 prostate cancer cells. Biochimica et Biophysica Acta (BBA) - Molecular and Cell Biology of Lipids. 2013;1831(7):1302-1309. doi:10.1016/j.bbalip.2013.04.011
56. Bellotti C, Stäuble A, Steinfeld R. CD9 and folate receptor overexpression are not sufficient for VSV-G-independent lentiviral transduction. PLoS One. 2022;17(3):e0264642. doi:10.1371/journal.pone.0264642
57. Ovchinnikova LA, Filimonova IN, Zakharova MY, et al. Targeting Extracellular Vesicles to Dendritic Cells and Macrophages. Acta Naturae. 2021;13(3):114-121. doi:10.32607/actanaturae.11478
58. Hagey DW, Ojansivu M, Bostancioglu BR, et al. The cellular response to extracellular vesicles is dependent on their cell source and dose. Sci Adv. 2023;9(35). doi:10.1126/sciadv.adh1168

59. Syromiatnikova V, Prokopeva A, Gomzikova M. Methods of the Large-Scale Production of Extracellular Vesicles. Int J Mol Sci. 2022;23(18):10522. doi:10.3390/ijms231810522
60. Roefs MT, Bauzá-Martinez J, van de Wakker SI, et al. Cardiac progenitor cell-derived extracellular vesicles promote angiogenesis through both associated- and co-isolated proteins. Commun Biol. 2023;6(1):800. doi:10.1038/s42003-023-05165-7
61. Vrijsen KR, Sluijter JPG, Schuchardt MWL, et al. Cardiomyocyte progenitor cell-derived exosomes stimulate migration of endothelial cells. J Cell Mol Med. Published online May 2010:no-no. doi:10.1111/j.1582-4934.2010.01081.x
62. Ridley AJ. Rho GTPases and actin dynamics in membrane protrusions and vesicle trafficking. Trends Cell Biol. 2006;16(10):522-529. doi:10.1016/j.tcb.2006.08.006
63. Chen S, Shiesh SC, Lee GB, Chen C. Two-step magnetic bead-based (2MBB) techniques for immunocapture of extracellular vesicles and quantification of microRNAs for cardiovascular diseases: A pilot study. PLoS One. 2020;15(2):e0229610. doi:10.1371/journal.pone.0229610
64. Cheng Y, Zeng Q, Han Q, Xia W. Effect of pH, temperature and freezing-thawing on quantity changes and cellular uptake of exosomes. Protein Cell. 2019;10(4):295-299. doi:10.1007/s13238-018-0529-4
65. Santos MF, Rappa G, Karbanová J, et al. Anti-human CD9 antibody Fab fragment impairs the internalization of extracellular vesicles and the nuclear transfer of their cargo proteins. J Cell Mol Med. 2019;23(6):4408-4421. doi:10.1111/jcmm.14334
66. Mangeot PE, Dollet S, Girard M, et al. Protein Transfer Into Human Cells by VSV-G-induced Nanovesicles. Molecular Therapy. 2011;19(9):1656-1666. doi:10.1038/mt.2011.138
67. Bernhardt HS, Tate WP. Primordial soup or vinaigrette: did the RNA world evolve at acidic pH? Biol Direct. 2012;7(1):4. doi:10.1186/1745-6150-7-4
68. Farrants H, Tarnawski M, Müller TG, et al. Chemogenetic Control of Nanobodies. Nat Methods. 2020;17(3):279-282. doi:10.1038/s41592-020-0746-7
69. Somiya M, Kuroda S. Real-Time Luminescence Assay for Cytoplasmic Cargo Delivery of Extracellular Vesicles. Anal Chem. 2021;93(13):5612-5620. doi:10.1021/acs.analchem.1c00339

# 6

# ANNEXES

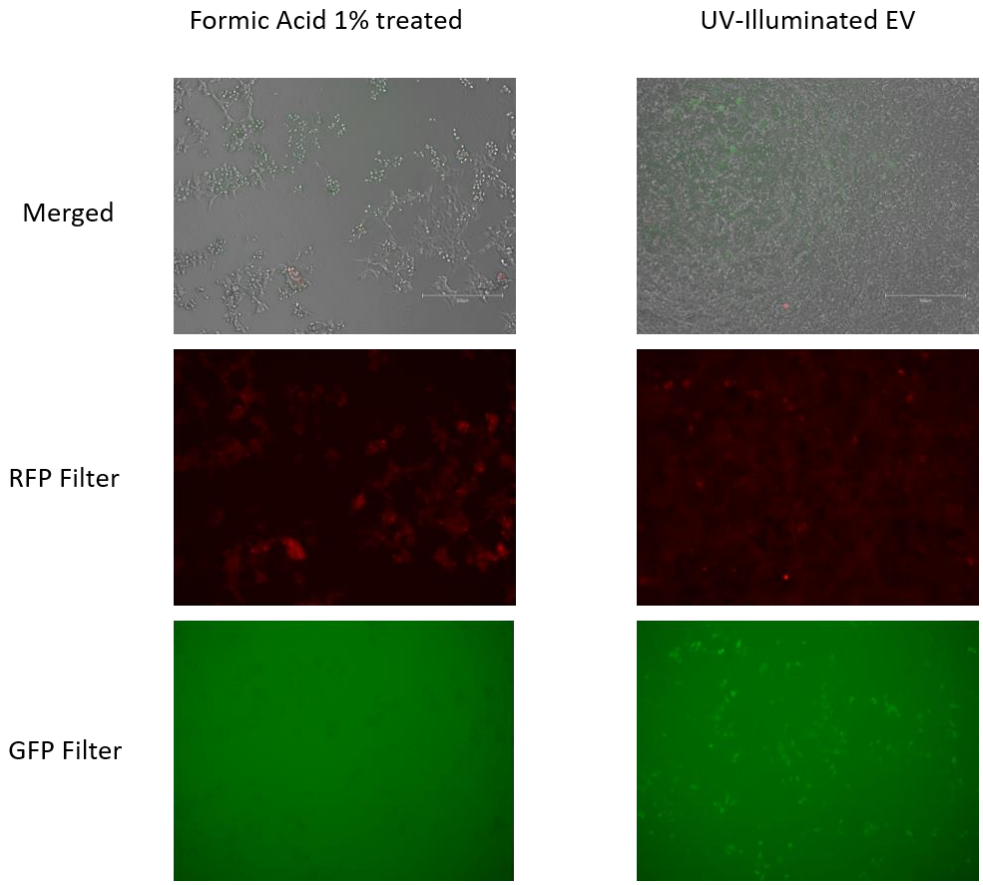


Figure 6.1. Fluorescent microscopy images taken of the cells treated with EVs, with the RFP and GFP filter at 100x magnification. On the left EV were treated with Formic acid 1% for 5 minutes and UV-illuminated. On the right EVs were illuminated only and added to the reporter cells.

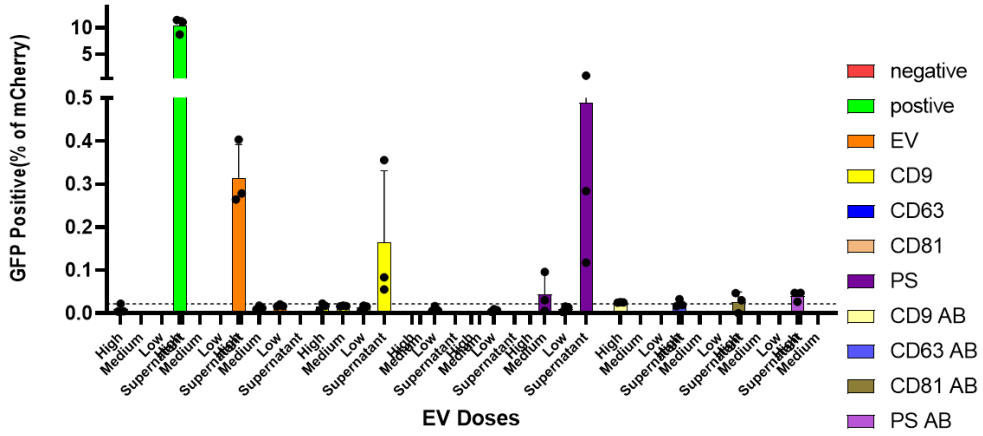


Figure 6.2. Myr enriched EVs only show supernatant activation. The functionality of EV subpopulations derived from HEK293T cells transfected with plasmids encoding for VSV-G, Cas9, sgRNA with MS2 aptamers and Myr-PhoCl-MS2 added in three doses (low= 3489.94, medium= 6979.88, high= 13959.77 Memglow590-derived fluorescence) to HEK293T stoplight cells was analyzed by eGFP expression by flow cytometry 3 days after addition of the samples. Supernatant samples (SP), obtained after isolation the specific subpopulation and antibody controls (AB) done by incubating the EV sample with the subpopulation antibody and the SHOBS elution buffer were added to the HEK293TSL reporter cells in the same concentration as the highest dose of the EV stock.